**Forecast reconciliation: Methodological issues and applications**

Chapter 5 - Cross-temporal probabilistic forecast reconciliation[1]

# Online appendix

**Candidate:** Daniele Girolimetto
**Supervisors:** Prof. Tommaso Di Fonzo, Prof. George Athanasopoulos and Prof. Rob J Hyndman

## Contents



[1]Girolimetto, D., Athanasopoulos, G., Di Fonzo, T. and Hyndman, R. J. (2023) Cross- temporal probabilistic forecast reconciliation: Methodological and practical issues. International Journal of Forecasting (in press). doi:10.1016/j.ijforecast.2023.10.003

# A Cross-sectional, temporal and cross-temporal covariance approximations

Table A.1 presents some approximations for the cross-sectional (Hyndman et al. 2011, 2016, Wickramasuriya et al. 2019) and the temporal (Athanasopoulos et al. 2017, Nystrup et al. 2020) covariance matrices. Di Fonzo & Girolimetto (2023*a*) consider the following approximations for the cross-temporal covariance matrix.

oct($ols$) - identity: $\boldsymbol{\Omega}_{ct} = \boldsymbol{I}_{n(k^*+m)}$.

oct($struc$) - structural: $\boldsymbol{\Omega}_{ct} = \text{diag}(\boldsymbol{S}_{ct}\mathbf{1}_{mn_b})$.

oct($wlsv$) - series variance scaling: $\boldsymbol{\Omega}_{ct} = \widehat{\boldsymbol{\Omega}}_{ct,wlsv}$, a straightforward extension of the series variance scaling matrix presented by Athanasopoulos et al. (2017).

oct($bdshr$) - block-diagonal shrunk cross-covariance scaling: $\boldsymbol{\Omega}_{ct} = \boldsymbol{P}\widehat{\boldsymbol{W}}^{BD}_{ct,shr}\boldsymbol{P}'$, with $\widehat{\boldsymbol{W}}^{BD}_{ct,shr}$ a block diagonal matrix where each $k-$block ($k = m, k_{p-1}, \dots, 1$) is $\boldsymbol{I}_{M_k} \otimes \widehat{\boldsymbol{W}}^{[k]}_{shr}$, $\widehat{\boldsymbol{W}}^{[k]}_{shr}$ is the shrunk estimate of the cross-sectional covariance matrix proposed by Wickramasuriya et al. (2019), and $\boldsymbol{P}$ is the commutation matrix such that $\boldsymbol{P}\text{vec}(\boldsymbol{Y}_\tau) = \text{vec}(\boldsymbol{Y}'_\tau)$.

oct($shr$) - MinT-shr: $\boldsymbol{\Omega}_{ct} = \hat{\lambda}\widehat{\boldsymbol{\Omega}}_{ct,D} + (1-\hat{\lambda})\widehat{\boldsymbol{\Omega}}_{ct}$, where $\hat{\lambda}$ is an estimated shrinkage coefficient (Ledoit & Wolf 2004), $\widehat{\boldsymbol{\Omega}}_{ct,D} = \boldsymbol{I}_{n(k^*+m)} \odot \widehat{\boldsymbol{\Omega}}_{ct}$ with $\odot$ denoting the Hadamard product, and $\widehat{\boldsymbol{\Omega}}_{ct}$ is the covariance matrix of the cross-temporal one-step ahead in-sample forecast errors.

oct($sam$) - MinT-sam: $\boldsymbol{\Omega}_{ct} = \widehat{\boldsymbol{\Omega}}_{ct}$.

| | **Cross-sectional framework** | **Temporal framework** |
|---|---|---|
| identity | cs($ols$): $\boldsymbol{W} = \boldsymbol{I}_n$ | te($ols$): $\boldsymbol{\Omega} = \boldsymbol{I}_{k^*+m}$ |
| structural | cs($struc$): $\boldsymbol{W} = \text{diag}(\boldsymbol{S}_{cs}\mathbf{1}_{nb})$ | te($struc$): $\boldsymbol{\Omega} = \text{diag}(\boldsymbol{S}_{te}\mathbf{1}_m)$ |
| series variance | cs($wls$): $\boldsymbol{W} = \widehat{\boldsymbol{W}}_D = \boldsymbol{I}_n \odot \widehat{\boldsymbol{W}}$ | te($wlsv$): $\boldsymbol{\Omega} = \widehat{\boldsymbol{\Omega}}_{wlsv}$ |
| MinT-shr | cs($shr$): $\boldsymbol{W} = \hat{\lambda}\widehat{\boldsymbol{W}}_D + (1-\hat{\lambda})\widehat{\boldsymbol{W}}$ | te($shr$): $\boldsymbol{\Omega} = \hat{\lambda}\widehat{\boldsymbol{\Omega}}_D + (1-\hat{\lambda})\widehat{\boldsymbol{\Omega}}$ |
| MinT-sam | cs($sam$): $\boldsymbol{W} = \widehat{\boldsymbol{W}}$ | te($sam$): $\boldsymbol{\Omega} = \widehat{\boldsymbol{\Omega}}$ |

**Note:** $\widehat{\boldsymbol{W}}$ ($\widehat{\boldsymbol{\Omega}}$) is the covariance matrix of the cross-sectional (temporal) one-step ahead in-sample forecast errors, $\widehat{\boldsymbol{\Omega}}_{wlsv}$ is a diagonal matrix presented by Athanasopoulos et al. (2017), and $\widehat{\boldsymbol{\Omega}}_D = \boldsymbol{I}_{k^*+m} \odot \widehat{\boldsymbol{\Omega}}$, where $\odot$ denotes the Hadamard product.

**Table A.1:** *Approximations for cross-sectional ($\boldsymbol{W}$) and temporal ($\boldsymbol{\Omega}$) covariance matrices.*

## B Alternative forms of the cross-temporal covariance matrix

In this appendix, some derivations of the solutions proposed in Section 4 to obtain an estimator of the cross-temporal covariance matrix are reported. Starting from the the definition of cross-temporal covariance matrix we obtain the first equivalence in (10). Therefore, we have that

$$\begin{aligned}
&\lambda\widehat{\boldsymbol{\Omega}}_{hf\text{-}bts,D} + (1-\lambda)\widehat{\boldsymbol{\Omega}}_{hf\text{-}bts} \\
&\qquad\Downarrow \\
&\widehat{\boldsymbol{\Omega}}_{HB} = \boldsymbol{S}_{ct}\left[\lambda\widehat{\boldsymbol{\Omega}}_{hf\text{-}bts,D} + (1-\lambda)\widehat{\boldsymbol{\Omega}}_{hf\text{-}bts}\right]\boldsymbol{S}_{ct}' \\
&\qquad\quad = \lambda\boldsymbol{S}_{ct}\widehat{\boldsymbol{\Omega}}_{hf\text{-}bts,D}\boldsymbol{S}_{ct}' + (1-\lambda)\boldsymbol{S}_{ct}\widehat{\boldsymbol{\Omega}}_{hf\text{-}bts}\boldsymbol{S}_{ct}'.
\end{aligned}$$

The high-frequency time series representation (the second equivalence) can be derived in the following manner:

$$\begin{aligned}
\widetilde{\boldsymbol{\Omega}} &= \boldsymbol{S}_{ct}\boldsymbol{\Omega}_{hf\text{-}bts}\boldsymbol{S}_{ct}' \\
&= (\boldsymbol{S}_{cs}\otimes\boldsymbol{S}_{te})\,\boldsymbol{\Omega}_{hf\text{-}bts}\,(\boldsymbol{S}_{cs}\otimes\boldsymbol{S}_{te})' \\
&= (\boldsymbol{I}_n\otimes\boldsymbol{S}_{te})\,(\boldsymbol{S}_{cs}\otimes\boldsymbol{I}_{m+k^*})\,\boldsymbol{\Omega}_{hf\text{-}bts}\,(\boldsymbol{S}_{cs}\otimes\boldsymbol{I}_{m+k^*})'\,(\boldsymbol{I}_n\otimes\boldsymbol{S}_{te})' \\
&= (\boldsymbol{I}_n\otimes\boldsymbol{S}_{te})\,\boldsymbol{\Omega}_{hf}\,(\boldsymbol{I}_n\otimes\boldsymbol{S}_{te})'
\end{aligned}$$

where $\boldsymbol{\Omega}_{hf} = (\boldsymbol{S}_{cs}\otimes\boldsymbol{I}_{m+k^*})\,\boldsymbol{\Omega}_{hf\text{-}bts}\,(\boldsymbol{S}_{cs}\otimes\boldsymbol{I}_{m+k^*})'$ and $\boldsymbol{S}_{ct} = \boldsymbol{S}_{cs}\otimes\boldsymbol{S}_{te} = (\boldsymbol{I}_n\otimes\boldsymbol{S}_{te})\,(\boldsymbol{S}_{cs}\otimes\boldsymbol{I}_{m+k^*})$. We can apply the shrinkage estimator as

$$\begin{aligned}
&\lambda\widehat{\boldsymbol{\Omega}}_{hf,D} + (1-\lambda)\widehat{\boldsymbol{\Omega}}_{hf} \\
&\qquad\Downarrow \\
&\widehat{\boldsymbol{\Omega}}_{H} = (\boldsymbol{I}_n\otimes\boldsymbol{S}_{te})\left[\lambda\widehat{\boldsymbol{\Omega}}_{hf,D} + (1-\lambda)\widehat{\boldsymbol{\Omega}}_{hf}\right](\boldsymbol{I}_n\otimes\boldsymbol{S}_{te})' \\
&\qquad\quad = \lambda(\boldsymbol{I}_n\otimes\boldsymbol{S}_{te})\widehat{\boldsymbol{\Omega}}_{hf,D}(\boldsymbol{I}_n\otimes\boldsymbol{S}_{te})' + (1-\lambda)(\boldsymbol{I}_n\otimes\boldsymbol{S}_{te})\widehat{\boldsymbol{\Omega}}_{hf}(\boldsymbol{I}_n\otimes\boldsymbol{S}_{te})'.
\end{aligned}$$

The bottom time series representation (the third equivalence) follows by

$$\begin{aligned}
\widetilde{\boldsymbol{\Omega}} &= \boldsymbol{S}_{ct}\boldsymbol{\Omega}_{hf\text{-}bts}\boldsymbol{S}_{ct}' \\
&= (\boldsymbol{S}_{cs}\otimes\boldsymbol{S}_{te})\,\boldsymbol{\Omega}_{hf\text{-}bts}\,(\boldsymbol{S}_{cs}\otimes\boldsymbol{S}_{te})' \\
&= (\boldsymbol{S}_{cs}\otimes\boldsymbol{I}_{m+k^*})\,(\boldsymbol{I}_n\otimes\boldsymbol{S}_{te})\,\boldsymbol{\Omega}_{hf\text{-}bts}\,(\boldsymbol{I}_n\otimes\boldsymbol{S}_{te})'\,(\boldsymbol{I}_n\otimes\boldsymbol{S}_{te})' \\
&= (\boldsymbol{S}_{cs}\otimes\boldsymbol{I}_{m+k^*})\,\boldsymbol{\Omega}_{bts}\,(\boldsymbol{S}_{cs}\otimes\boldsymbol{I}_{m+k^*})',
\end{aligned}$$

where $\boldsymbol{\Omega}_{bts} = (\boldsymbol{I}_n\otimes\boldsymbol{S}_{te})\,\boldsymbol{\Omega}_{hf\text{-}bts}\,(\boldsymbol{I}_n\otimes\boldsymbol{S}_{te})'$ and $\boldsymbol{S}_{ct} = \boldsymbol{S}_{cs}\otimes\boldsymbol{S}_{te} = (\boldsymbol{S}_{cs}\otimes\boldsymbol{I}_{m+k^*})\,(\boldsymbol{I}_n\otimes\boldsymbol{S}_{te})$. Finally we have that

$$\begin{aligned}
&\lambda\widehat{\boldsymbol{\Omega}}_{bts,D} + (1-\lambda)\widehat{\boldsymbol{\Omega}}_{bts} \\
&\qquad\Downarrow \\
&\widehat{\boldsymbol{\Omega}}_{B} = (\boldsymbol{S}_{cs}\otimes\boldsymbol{I}_{m+k^*})\left[\lambda\widehat{\boldsymbol{\Omega}}_{bts,D} + (1-\lambda)\widehat{\boldsymbol{\Omega}}_{bts}\right](\boldsymbol{S}_{cs}\otimes\boldsymbol{I}_{m+k^*})' \\
&\qquad\quad = \lambda\,(\boldsymbol{S}_{cs}\otimes\boldsymbol{I}_{m+k^*})\,\widehat{\boldsymbol{\Omega}}_{bts,D}\,(\boldsymbol{S}_{cs}\otimes\boldsymbol{I}_{m+k^*})' +
\end{aligned}$$

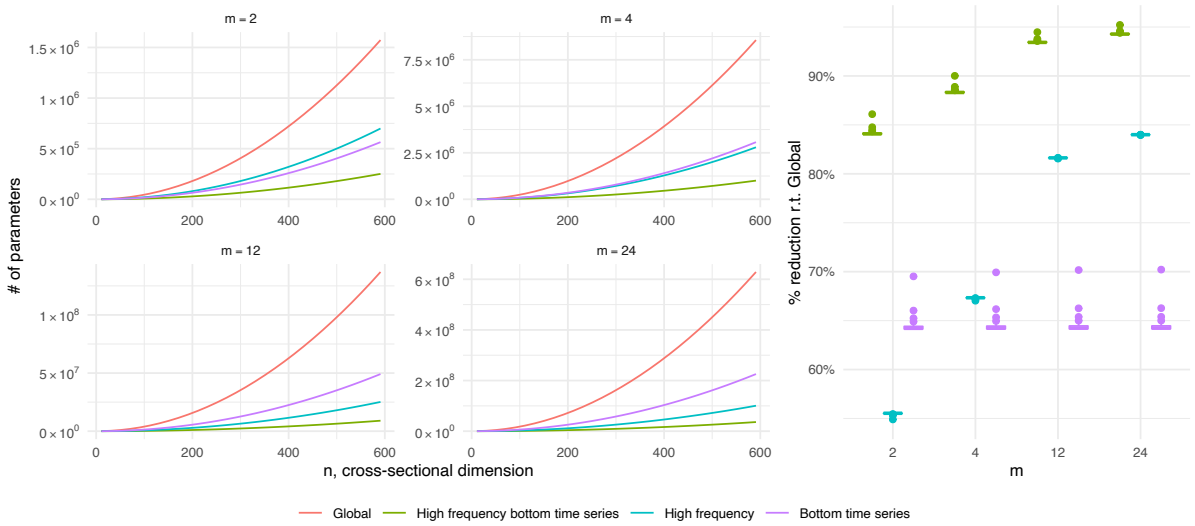


**Figure B.1:** *The four graphs on the left represent the number of different parameters in the covariance matrix for the various approaches presented for different values of m and n ($n_b$, the number of bottom time series, is about 60% of the total). On the right, we have the boxplot of the percentage reduction in the number of parameters compared to the global approach.*

$$(1-\lambda)\left(\boldsymbol{S}_{cs}\otimes\boldsymbol{I}_{m+k^*}\right)\widehat{\boldsymbol{\Omega}}_{bts}\left(\boldsymbol{S}_{cs}\otimes\boldsymbol{I}_{m+k^*}\right)'.$$

In general, the covariance matrix of the reconciled forecasts is equal to $\boldsymbol{M}\widehat{\boldsymbol{\Omega}}\boldsymbol{M}'$ where $\boldsymbol{M}=\boldsymbol{S}_{ct}\boldsymbol{G}$ is the projection matrix. When using the HB approach, the covariance matrix of the reconciliation and the base forecasts will be identical. Indeed, it can be shown (see Panagiotelis et al. 2021 for more details) that if $\boldsymbol{M}$ is a projection matrix (6) then $\boldsymbol{M}\boldsymbol{S}_{ct}=\boldsymbol{S}_{ct}\boldsymbol{G}\boldsymbol{S}_{ct}=\boldsymbol{S}_{ct}$, and we obtain that

$$\begin{aligned}\boldsymbol{M}\widehat{\boldsymbol{\Omega}}_{HB}\boldsymbol{M}' &= \boldsymbol{M}\boldsymbol{S}_{ct}\widehat{\boldsymbol{\Omega}}_{\text{hf-bts},HB}\boldsymbol{S}_{ct}'\boldsymbol{M}'\\ &= \boldsymbol{S}_{ct}\boldsymbol{G}\boldsymbol{S}_{ct}\widehat{\boldsymbol{\Omega}}_{\text{hf-bts},HB}\boldsymbol{S}_{ct}'\boldsymbol{G}'\boldsymbol{S}_{ct}'\\ &= \boldsymbol{S}_{ct}\widehat{\boldsymbol{\Omega}}_{\text{hf-bts},HB}\boldsymbol{S}_{ct}'=\widehat{\boldsymbol{\Omega}}_{HB}.\end{aligned}$$

Figure B.1 shows the number of parameters for different values of $m$ and $n$, with $n_b$ fixed to approximately 60% of $n$. The right panel reports the boxplot of the percentage reductions in the number of parameters compared to the global approach. Figure B.2 gives some visual insights on the covariance matrices obtainable with $\lambda=0$ and $\lambda=1$, respectively, for a simple cross-temporal hierarchical structure with 3 time series and $\mathcal{K}=\{2,1\}$ (e.g, cross-temporal semi-annual, see the Monte Carlo simulation in Appendix C).

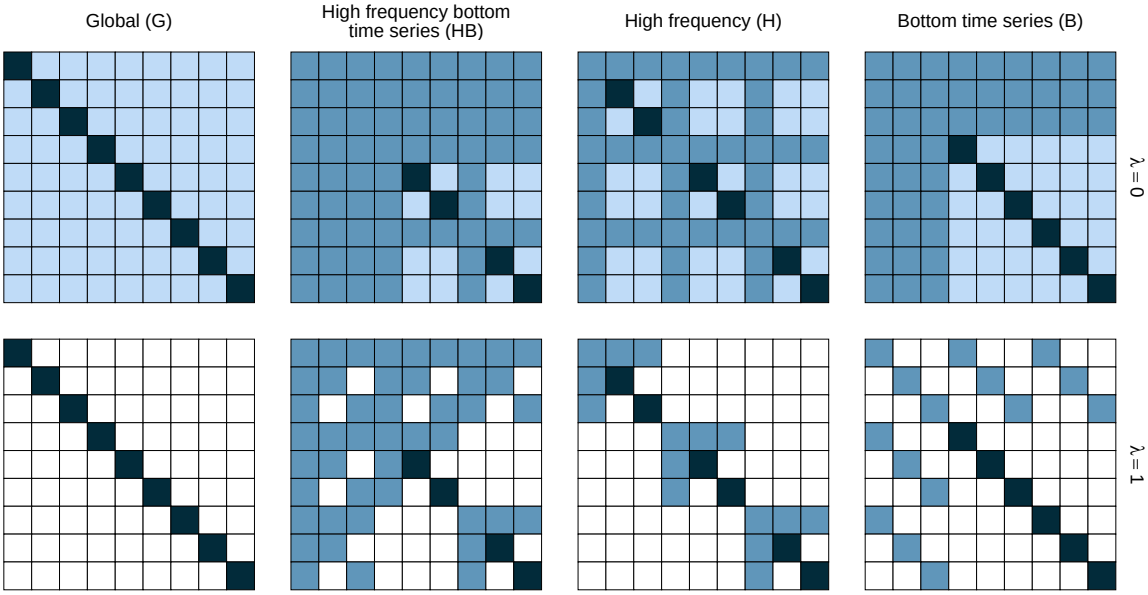


**Figure B.2:** *Representation of four types of covariance matrices that can be obtained from the cross-temporal hierarchical structure (3 time series and $m = 2$) for two different values of $\lambda \in \{0, 1\}$, the shrinkage parameter. The cells that are not modified by shrinkage are colored black, those actively involved in the shrinkage phase are colored light blue, and those derived from and not estimated by the base forecasts errors are colored blue. Additionally, for $\lambda = 1$, the cells corresponding to a zero value are colored white.*

## B.1 Proof Theorem 4.1

*Proof.* Let $\boldsymbol{S}_{ct}^{+} = (\boldsymbol{S}_{ct}'\boldsymbol{S}_{ct})^{-1}\boldsymbol{S}_{ct}'$ be the generalized inverse of $\boldsymbol{S}_{ct}$ ($\boldsymbol{S}_{ct}$ has linearly independent columns by construction). Applying (6), we obtain

$$\widetilde{\boldsymbol{b}}_{ols}^{[1]} = (\boldsymbol{S}_{ct}'\boldsymbol{S}_{ct})^{-1}\boldsymbol{S}_{ct}'\widehat{\boldsymbol{x}}_h$$

and

$$\widetilde{\boldsymbol{b}}_{hb}^{[1]} = [\boldsymbol{S}_{ct}'(\boldsymbol{S}_{ct}\widehat{\boldsymbol{\Omega}}_{hf-bts}\boldsymbol{S}_{ct}')^{+}\boldsymbol{S}_{ct}]^{-1}\boldsymbol{S}_{ct}'(\boldsymbol{S}_{ct}\widehat{\boldsymbol{\Omega}}_{hf-bts}\boldsymbol{S}_{ct}')^{+}\widehat{\boldsymbol{x}}_h.$$

Since $(\boldsymbol{AB})^{+} = \boldsymbol{B}^{+}\boldsymbol{A}^{+}$ (**?**), then

$$\begin{aligned}\boldsymbol{S}_{ct}'(\boldsymbol{S}_{ct}\widehat{\boldsymbol{\Omega}}_{hf-bts}\boldsymbol{S}_{ct}')^{+}\boldsymbol{S}_{ct} &= \boldsymbol{S}_{ct}'(\widehat{\boldsymbol{\Omega}}_{hf-bts}^{1/2}\boldsymbol{S}_{ct}')^{+}(\boldsymbol{S}_{ct}\widehat{\boldsymbol{\Omega}}_{hf-bts}^{1/2})^{+}\boldsymbol{S}_{ct} \\ &= \boldsymbol{S}_{ct}'(\boldsymbol{S}_{ct}')^{+}\widehat{\boldsymbol{\Omega}}_{hf-bts}^{+}\boldsymbol{S}_{ct}^{+}\boldsymbol{S}_{ct} = \widehat{\boldsymbol{\Omega}}_{hf-bts}^{+} = \widehat{\boldsymbol{\Omega}}_{hf-bts}^{-1}\end{aligned} \tag{B.1}$$

and

$$\begin{aligned}\boldsymbol{S}_{ct}'(\boldsymbol{S}_{ct}\widehat{\boldsymbol{\Omega}}_{hf-bts}\boldsymbol{S}_{ct}')^{+} &= \boldsymbol{S}_{ct}'(\widehat{\boldsymbol{\Omega}}_{hf-bts}^{1/2}\boldsymbol{S}_{ct}')^{+}(\boldsymbol{S}_{ct}\widehat{\boldsymbol{\Omega}}_{hf-bts}^{1/2})^{+} \\ &= \widehat{\boldsymbol{\Omega}}_{hf-bts}^{-1}\boldsymbol{S}_{ct}^{+} = \widehat{\boldsymbol{\Omega}}_{hf-bts}^{-1}(\boldsymbol{S}_{ct}'\boldsymbol{S}_{ct})^{-1}\boldsymbol{S}_{ct}'.\end{aligned} \tag{B.2}$$

Therefore,

$$\begin{aligned}\widetilde{\boldsymbol{b}}_{hb}^{[1]} &= [\boldsymbol{S}_{ct}'(\boldsymbol{S}_{ct}\widehat{\boldsymbol{\Omega}}_{hf-bts}\boldsymbol{S}_{ct}')^{+}\boldsymbol{S}_{ct}]^{-1}\boldsymbol{S}_{ct}'(\boldsymbol{S}_{ct}\widehat{\boldsymbol{\Omega}}_{hf-bts}\boldsymbol{S}_{ct}')^{+}\widehat{\boldsymbol{x}}_h \\ &\overset{(B.1)}{=} \widehat{\boldsymbol{\Omega}}_{hf-bts}\boldsymbol{S}_{ct}'(\boldsymbol{S}_{ct}\widehat{\boldsymbol{\Omega}}_{hf-bts}\boldsymbol{S}_{ct}')^{+}\widehat{\boldsymbol{x}}_h \\ &\overset{(B.2)}{=} \widehat{\boldsymbol{\Omega}}_{hf-bts}\widehat{\boldsymbol{\Omega}}_{hf-bts}^{-1}(\boldsymbol{S}_{ct}'\boldsymbol{S}_{ct})^{-1}\boldsymbol{S}_{ct}'\widehat{\boldsymbol{x}}_h \\ &= (\boldsymbol{S}_{ct}'\boldsymbol{S}_{ct})^{-1}\boldsymbol{S}_{ct}'\widehat{\boldsymbol{x}}_h = \widetilde{\boldsymbol{b}}_{ols}^{[1]}\end{aligned}$$

□

# C Monte Carlo simulation

We study the effect of combining cross-sectional and temporal aggregations, using a simple hierarchy that allows us to effectively visualize the quantities involved, such as the covariance matrix. Additionally, the small size and nature of the data generating process make it possible to exactly calculate the true cross-temporal covariance structure, thus providing insights into the nature of the time series data involved in the forecast reconciliation process.

Consider a 2-level hierarchical structure with three time series (one upper series, $A$, and two bottom series, $B$ and $C$) such that the cross-sectional aggregation matrix is $\boldsymbol{A}_{cs} = [1 \quad 1]$ ($A = B + C$). The temporal structure we are considering is equivalent to using semi-annual data with $\mathcal{K} = \{2, 1\}$ and $m = 2$. The assumed Data-Generating Processes (DPG) for the semi-annual bottom level series are two AR(2) given by

$$y_{B,t} = \phi_{B,1} y_{B,t-1} + \phi_{B,2} y_{B,t-2} + \varepsilon_{B,t}$$
$$y_{C,t} = \phi_{C,1} y_{C,t-1} + \phi_{C,2} y_{C,t-2} + \varepsilon_{C,t}$$

with parameters[2] $\boldsymbol{\phi}_B = [\phi_{B,1} \ \phi_{B,2}]' = [1.34 \ -0.74]'$ and $\boldsymbol{\phi}_C = [\phi_{C,1} \ \phi_{C,2}]' = [0.95 \ -0.42]'$. The error $\boldsymbol{\varepsilon}_t = [\varepsilon_{B,t} \quad \varepsilon_{C,t}]'$ driving the process is drawn from a multivariate normal distribution with standard deviations simulated from a uniform distribution between 0.5 and 2 and a fixed correlation of -0.8. The cross-sectional error covariance matrix is thus given by

$$\boldsymbol{\Omega}_{cs} = \begin{bmatrix} 0.9 & 0 \\ 0 & 1.8 \end{bmatrix} \begin{bmatrix} 1 & \rho \\ \rho & 1 \end{bmatrix} \begin{bmatrix} 0.9 & 0 \\ 0 & 1.8 \end{bmatrix} = \begin{bmatrix} \sigma_B^2 & \sigma_{BC} \\ \sigma_{BC} & \sigma_C^2 \end{bmatrix}.$$

To obtain the remaining series, the bottom series are then cross-temporally aggregated.

For the forecast experiment, the base forecasts are computing using AR models where the order is automatically determined by the algorithm proposed by Hyndman & Khandakar (2008) and implemented in the R package `forecast` (Hyndman et al. 2023), thus allowing for possible mis-specification in the models. The training window length is 500 years, consisting of 1000 high frequency observations. The experiment is replicated 500 times, with a forecast horizon of 1 year.

Since the AR(2) models used as DPG for the bottom series $B$ and $C$ at the most disaggregated temporal level are known, we may compute the true covariance matrix for one-step ahead forecasts at the annual level $\boldsymbol{\Omega}_{ct} = \boldsymbol{S}_{ct} \boldsymbol{\Omega}_{hf\text{-}bts} \boldsymbol{S}_{ct}'$, where

$$\boldsymbol{\Omega}_{hf\text{-}bts} = \begin{bmatrix} \sigma_B^2 & & & \\ \phi_{B,1}\sigma_B^2 & \sigma_B^2\left(1+\phi_{B,1}^2\right) & & \\ \sigma_{BC} & \phi_{B,1}\sigma_{BC} & \sigma_C^2 & \\ \phi_{C,1}\sigma_{BC} & \sigma_{BC}\left(1+\phi_{B,1}\phi_{C,1}\right) & \phi_{C,1}\sigma_C^2 & \sigma_C^2\left(1+\phi_{C,1}^2\right) \end{bmatrix}.$$

The detailed calculations can be found in Section C.2. Figure C.3 shows both the covariance matrix and the correlation matrix for fixed parameters.

[2]The $\boldsymbol{\phi}_B$ and $\boldsymbol{\phi}_C$ parameters are estimated from the "Lynx" and "Hare" time series contained in the `pelt` dataset of the `tsibbledata` package for R (O'Hara-Wild et al. 2022).

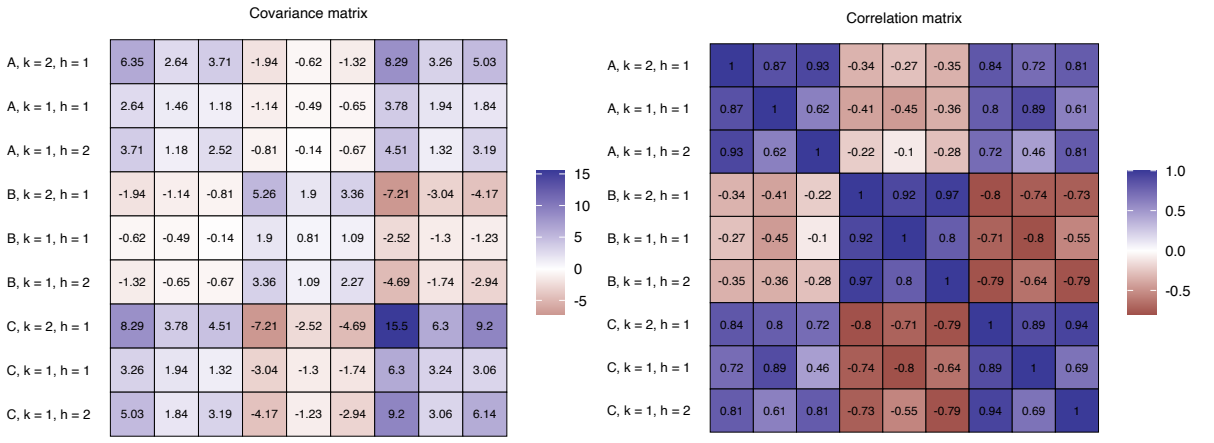


**Figure C.3:** *Simulation experiment. True cross-temporal covariance (left) and correlation (right) error matrix of the reconciled forecasts with* $\sigma_B = 0.9$, $\sigma_C = 1.8$, $\boldsymbol{\phi}_B = [1.34 \ -0.74]'$, $\boldsymbol{\phi}_C = [0.95 \ -0.42]'$ *and* $\rho = -0.8$.

To construct cross-temporal samples of the base forecasts, we use the Gaussian and bootstrap approaches discussed in Sections 3.1 and 3.2, respectively. For the parametric approach we use multi-step residuals with the different covariance matrix structures analyzed in 4.1, while for the non-parametric approach, we use regular one-step residuals. We do not use overlapping residuals in our analysis as we have the advantage of generating a large number of observation. Ten different reconciliation approaches have been adopted (see Table 2): $\text{ct}(bu)$, $\text{ct}(shr_{cs}, bu_{te})$, $\text{ct}(wlsv_{te}, bu_{cs})$, $\text{oct}(wlsv)$, $\text{oct}(bdshr)$, $\text{oct}_h(shr)$, $\text{oct}_h(bshr)$, and $\text{oct}_h(hshr)$.

## C.1 Covariance matrix comparison and forecast accuracy scores

To compare the true covariance matrix $\boldsymbol{\Omega}_{ct}$ with the estimated covariance matrix $\widehat{\boldsymbol{\Omega}}$, we use the Frobenius norm to quantify the difference between two matrices:

$$\|\boldsymbol{D}\|_F = \sqrt{\sum_{i=1}^{n(k^*+m)} \sum_{j=1}^{n(k^*+m)} |d_{i,j}|^2}$$

where $\boldsymbol{D} = \widehat{\boldsymbol{\Omega}} - \boldsymbol{\Omega}_{ct}$. The true covariance matrix, shown in Figure C.3, was compared to the estimated covariance matrices obtained using various reconciliation approaches and techniques for generating sample paths of the base forecasts. Thus, we should be able to determine which reconciliation approach and simulation technique produce an accurate estimate of the covariance matrix. Other types of matrix norms were also considered with similar results.

From Table C.1, it appears that the reconciled covariance matrices are always closer to the true matrix than the base forecast matrix when using both the Gaussian and the bootstrap approach. Overall, there are no major differences in the findings when using either one-step or multi-step residuals in cross-temporal forecast reconciliation. In fact, using approaches like $\text{oct}(bdshr)$, we obtain results that are consistent with approaches such as $\text{oct}_h(shr)$, where no temporal and/or cross-sectional correlation assumptions are imposed. It is worth noting that the $HB$ covariance matrix when used to calculate the base forecasts samples, is not changed by the reconciliation step (see Appendix B). In conclusion, our results suggest that using multi-step

| Reconciliation approach | Generation of the base forecasts paths | | | | |
|---|---|---|---|---|---|
| | ctjb | Gaussian approach* | | | |
| | | G | B | H | HB |
| base | 8.260 | 7.748 | 6.549 | 3.409 | 2.215 |
| ct($bu$) | 3.195 | 2.215 | 2.215 | **2.215** | 2.215 |
| ct($shr_{cs}, bu_{te}$) | 3.202 | 2.224 | 2.215 | 2.224 | 2.215 |
| ct($wlsv_{te}, bu_{cs}$) | **3.183** | **2.188** | 2.188 | **2.215** | 2.215 |
| oct($wlsv$) | 3.766 | 3.082 | 2.191 | 2.910 | 2.215 |
| oct($bdshr$) | 3.203 | 2.195 | **2.184** | 2.224 | **2.215** |
| oct$_h$($shr$) | 3.251 | 2.260 | 2.202 | 2.226 | 2.215 |
| oct$_h$($bshr$) | 3.602 | 2.720 | 2.220 | 2.756 | 2.215 |
| oct$_h$($hshr$) | 4.869 | 4.138 | 4.167 | 2.225 | 2.215 |

*The Gaussian method employs a sample covariance with multi-step residuals.

**Table C.1:** *Simulation experiment. Frobenius norm between the true and the estimated covariance matrix for different reconciliation approaches and different techniques for simulating the base forecasts. Entries in bold represent the lowest value for each column, while the blue entry represent the global minimum. The reconciliation approaches are described in Table 2.*

residuals or bootstrap techniques may help find a "good" estimate of the covariance matrix, which can be further improved by the reconciliation.

A limitation of this simulation setting is that we are using a high number of residuals, which may result in undervaluing the benefit from using the parameterization form of the covariance matrix such as $HB$, $H$, or $B$ (see Section 4). Additionally, shrinkage techniques often yield very similar results when we use the corresponding matrix with $\lambda = 0$ (full covariance matrix).

In Tables C.2 and C.3 are reported the $\overline{\text{RelCRPS}}$ and ES ratio indices introduced in Sections 5 where low values indicate better quality of the forecasts. The good performance of the ct($bu$) approach can be explained by a good quality of the base forecasts at the bottom level for $k = 1$, and therefore it is difficult for the other approaches to correctly adjust them using the somewhat less good forecasts of the higher temporal and cross-sectional levels. This also explains the good performance of ct($shr_{cs}, bu_{te}$), which by definition only takes into account the information provided by the most temporally disaggregated base forecasts. Looking at the optimal cross-temporal reconciliation approaches, it does not seem to be any advantage in using multi-step residuals to calculate the covariance matrix in the reconciliation step.

In conclusion, we found that simulating base forecasts from multi-step residuals allows us to estimate a covariance matrix close to the true one. Additionally, we observed that reconciliation could be used to further improve the accuracy of these estimates: accurate base forecasts for $k = 1$ assist the good performance for bottom-up and optimal cross-temporal reconciliation approaches, such as oct($wlsv$) and oct($bdshr$), which perform well in terms of both CRPS and ES.

| Reconciliation approach | Generation of the base forecasts sample paths | | | | | | | | | |
|---|---|---|---|---|---|---|---|---|---|---|
| | ctjb | Gaussian approach* | | | | ctjb | Gaussian approach* | | | |
| | | G | B | H | HB | | G | B | H | HB |
| | $\forall k \in \{2,1\}$ | | | | | $k=1$ | | | | |
| base | 1.000 | 0.998 | 0.999 | 1.002 | 1.004 | 1.000 | 0.998 | 0.999 | 0.999 | 1.000 |
| ct($bu$) | 0.901 | 0.900 | 0.900 | 0.900 | 0.900 | 0.978 | 0.976 | 0.976 | 0.977 | 0.977 |
| ct($shr_{cs}, bu_{te}$) | **0.901** | **0.900** | **0.899** | **0.900** | **0.900** | **0.977** | **0.976** | **0.976** | **0.976** | **0.976** |
| ct($wlsv_{te}, bu_{cs}$) | 0.910 | 0.916 | 0.916 | 0.916 | 0.917 | 0.986 | 0.993 | 0.993 | 0.993 | 0.993 |
| oct($wlsv$) | 0.922 | 0.930 | 0.930 | 0.930 | 0.931 | 0.998 | 1.006 | 1.006 | 1.007 | 1.007 |
| oct($bdshr$) | 0.910 | 0.916 | 0.915 | 0.916 | 0.916 | 0.986 | 0.992 | 0.992 | 0.993 | 0.993 |
| oct$_h$($shr$) | 0.904 | 0.903 | 0.902 | 0.902 | 0.903 | 0.980 | 0.979 | 0.978 | 0.979 | 0.979 |
| oct$_h$($bshr$) | 0.923 | 0.922 | 0.922 | 0.921 | 0.922 | 0.999 | 0.998 | 0.998 | 0.998 | 0.998 |
| oct$_h$($hshr$) | 0.974 | 0.972 | 0.972 | 0.974 | 0.975 | 1.052 | 1.050 | 1.050 | 1.053 | 1.053 |
| | $k=2$ | | | | | | | | | |
| base | 1.000 | 0.998 | 0.999 | 1.005 | 1.008 | | | | | |
| ct($bu$) | 0.831 | 0.830 | 0.829 | 0.829 | 0.830 | | | | | |
| ct($shr_{cs}, bu_{te}$) | **0.830** | **0.830** | **0.829** | **0.829** | **0.830** | | | | | |
| ct($wlsv_{te}, bu_{cs}$) | 0.840 | 0.846 | 0.844 | 0.845 | 0.846 | | | | | |
| oct($wlsv$) | 0.851 | 0.859 | 0.859 | 0.859 | 0.861 | | | | | |
| oct($bdshr$) | 0.839 | 0.845 | 0.844 | 0.845 | 0.846 | | | | | |
| oct$_h$($shr$) | 0.834 | 0.833 | 0.831 | 0.832 | 0.832 | | | | | |
| oct$_h$($bshr$) | 0.852 | 0.851 | 0.851 | 0.851 | 0.852 | | | | | |
| oct$_h$($hshr$) | 0.902 | 0.900 | 0.899 | 0.901 | 0.902 | | | | | |

*The Gaussian method employs a sample covariance matrix and includes four techniques (G, B, H, HB) with multi-step residuals.

**Table C.2:** *Simulation experiment.* $\overline{RelCRPS}$ *defined in Section 5. Approaches performing worse than the benchmark (bootstrap base forecasts, ctjb) are highlighted in red, the best for each column is marked in bold, and the overall lowest value is highlighted in blue. The reconciliation approaches are described in Table 2.*

## C.2 Cross-temporal covariance matrix

We assume two AR(2) processes with correlated errors such that

$$y_{i,t} = \phi_{i,1} y_{i,t-1} + \phi_{i,2} y_{i,t-2} + \varepsilon_{i,t}$$

where $\boldsymbol{\varepsilon}_t \sim \mathcal{N}_2\left(\mathbf{0}_{(2\times 1)}, \boldsymbol{\Omega}_{cs}\right)$ and $i \in \{B, C\}$. Let $y_{i,T+h}$ be the true observation for the $i^{th}$ series and $\widetilde{y}_{i,T+h}$ the corresponding forecasts such that

$$\begin{aligned} y_{i,T+1} &= \phi_{i,1} y_{i,T} + \phi_{i,2} y_{i,T-1} + \varepsilon_{i,T+1} \\ y_{i,T+2} &= \phi_{i,1} y_{i,T+1} + \phi_{i,2} y_{i,T} + \varepsilon_{i,T+2} \end{aligned} \quad \text{and} \quad \begin{aligned} \widetilde{y}_{i,T+1} &= \phi_{i,1} y_{i,T} + \phi_{i,2} y_{i,T-1} \\ \widetilde{y}_{i,T+2} &= \phi_{i,1} \widetilde{y}_{i,T+1} + \phi_{i,2} y_{i,T} \end{aligned},$$

then

$$\begin{aligned} y_{i,T+1} - \widetilde{y}_{i,T+1} &= \varepsilon_{i,T+1} \\ y_{i,T+2} - \widetilde{y}_{i,T+2} &= \varepsilon_{i,T+2} + \phi_{i,1} \varepsilon_{i,T+1}. \end{aligned}$$

Finally, we can compute each element of the high frequency bottom time series covariance matrix

$$\begin{aligned} Var\left(y_{i,T+1} - \widetilde{y}_{i,T+1}\right) &= \sigma_i^2, \quad \forall i \in \{B, C\} \\ Var\left(y_{i,T+2} - \widetilde{y}_{i,T+2}\right) &= \sigma_i^2 \left(1 + \phi_{i,1}^2\right), \quad \forall i \in \{B, C\} \\ Cov\left[\left(y_{i,T+2} - \widetilde{y}_{i,T+2}\right), \left(y_{i,T+1} - \widetilde{y}_{i,T+1}\right)\right] &= Cov\left[\left(y_{i,T+1} - \widetilde{y}_{i,T+1}\right), \left(y_{i,T+2} - \widetilde{y}_{i,T+2}\right)\right] \end{aligned}$$

| Reconciliation approach | Generation of the base forecasts sample paths | | | | | | | | | |
|---|---|---|---|---|---|---|---|---|---|---|
| | ctjb | Gaussian approach* | | | | ctjb | Gaussian approach* | | | |
| | | G | B | H | HB | | G | B | H | HB |
| | $\forall k \in \{2,1\}$ | | | | | $k=1$ | | | | |
| base | 1.000 | 0.996 | 0.999 | 1.000 | 1.004 | 1.000 | 0.997 | 1.000 | 0.997 | 1.000 |
| ct($bu$) | 0.897 | 0.895 | 0.896 | 0.897 | **0.895** | 0.969 | **0.967** | **0.967** | 0.968 | **0.968** |
| ct($shr_{cs}, bu_{te}$) | **0.896** | **0.895** | **0.895** | **0.896** | 0.896 | **0.968** | 0.968 | 0.967 | **0.968** | 0.968 |
| ct($wlsv_{te}, bu_{cs}$) | 0.906 | 0.912 | 0.911 | 0.910 | 0.912 | 0.977 | 0.984 | 0.983 | 0.981 | 0.984 |
| oct($wlsv$) | 0.916 | 0.923 | 0.923 | 0.923 | 0.924 | 0.989 | 0.994 | 0.995 | 0.995 | 0.997 |
| oct($bdshr$) | 0.906 | 0.910 | 0.910 | 0.911 | 0.912 | 0.977 | 0.981 | 0.982 | 0.983 | 0.985 |
| oct$_h$($shr$) | 0.900 | 0.898 | 0.898 | 0.897 | 0.898 | 0.971 | 0.969 | 0.969 | 0.969 | 0.969 |
| oct$_h$($bshr$) | 0.916 | 0.914 | 0.916 | 0.915 | 0.916 | 0.987 | 0.986 | 0.987 | 0.987 | 0.988 |
| oct$_h$($hshr$) | 0.967 | 0.964 | 0.964 | 0.966 | 0.967 | 1.040 | 1.036 | 1.036 | 1.040 | 1.040 |
| | | | $k=2$ | | | | | | | |
| base | 1.000 | 0.996 | 0.998 | 1.003 | 1.008 | | | | | |
| ct($bu$) | 0.831 | 0.829 | 0.829 | 0.830 | **0.828** | | | | | |
| ct($shr_{cs}, bu_{te}$) | **0.829** | **0.828** | **0.829** | **0.829** | 0.829 | | | | | |
| ct($wlsv_{te}, bu_{cs}$) | 0.839 | 0.844 | 0.844 | 0.844 | 0.845 | | | | | |
| oct($wlsv$) | 0.849 | 0.858 | 0.856 | 0.856 | 0.857 | | | | | |
| oct($bdshr$) | 0.839 | 0.845 | 0.843 | 0.845 | 0.844 | | | | | |
| oct$_h$($shr$) | 0.835 | 0.833 | 0.833 | 0.831 | 0.832 | | | | | |
| oct$_h$($bshr$) | 0.850 | 0.847 | 0.849 | 0.849 | 0.850 | | | | | |
| oct$_h$($hshr$) | 0.900 | 0.897 | 0.896 | 0.897 | 0.899 | | | | | |

*The Gaussian method employs a sample covariance matrix and includes four techniques (G, B, H, HB) with multi-step residuals.

**Table C.3:** *Simulation experiment. ES ratio indices defined in Section 5. Approaches performing worse than the benchmark (bootstrap base forecasts, ctjb) are highlighted in red, the best for each column is marked in bold, and the overall lowest value is highlighted in blue. The reconciliation approaches are described in Table 2.*

$$
\begin{aligned}
& & &= \phi_{i,1}\sigma_i^2, \quad \forall i \in \{B,C\} \\
Cov\left[\left(y_{i,T+1}-\widetilde{y}_{i,T+1}\right),\left(y_{j,T+1}-\widetilde{y}_{j,T+1}\right)\right] &= Cov\left[\left(y_{j,T+1}-\widetilde{y}_{j,T+1}\right),\left(y_{i,T+1}-\widetilde{y}_{i,T+1}\right)\right] \\
& &= \sigma_{i,j}, \quad \forall i,j \in \{B,C\}, \quad i \neq j \\
Cov\left[\left(y_{i,T+2}-\widetilde{y}_{i,T+2}\right),\left(y_{j,T+1}-\widetilde{y}_{j,T+1}\right)\right] &= Cov\left[\left(y_{j,T+1}-\widetilde{y}_{j,T+1}\right),\left(y_{i,T+2}-\widetilde{y}_{i,T+2}\right)\right] \\
& &= \phi_{i,1}\sigma_{i,j}, \quad \forall i,j \in \{B,C\}, \quad i \neq j \\
Cov\left[\left(y_{i,T+2}-\widetilde{y}_{i,T+2}\right),\left(y_{j,T+2}-\widetilde{y}_{j,T+2}\right)\right] &= Cov\left[\left(y_{j,T+2}-\widetilde{y}_{j,T+2}\right),\left(y_{i,T+2}-\widetilde{y}_{i,T+2}\right)\right] \\
& &= \sigma_{i,j}\left(1+\phi_{i,1}\phi_{j,1}\right), \quad \forall i,j \in \{B,C\}, \quad i \neq j.
\end{aligned}
$$

In conclusion,

$$
\boldsymbol{\Omega}_{hf\text{-}bts} = \begin{bmatrix}
\sigma_B^2 & & & \\
\phi_{B,1}\sigma_B^2 & \sigma_B^2\left(1+\phi_{B,1}^2\right) & & \\
\sigma_{BC} & \phi_{B,1}\sigma_{BC} & \sigma_C^2 & \\
\phi_{C,1}\sigma_{BC} & \sigma_{BC}\left(1+\phi_{B,1}\phi_{C,1}\right) & \phi_{C,1}\sigma_C^2 & \sigma_C^2\left(1+\phi_{C,1}^2\right)
\end{bmatrix}
$$

and

$$
\boldsymbol{\Omega}_{ct} = \boldsymbol{S}_{ct}\boldsymbol{\Omega}_{hf\text{-}bts}\boldsymbol{S}_{ct}'.
$$

## C.3 One-step residuals and shrinkage covariance matrix

In Section 4.1, we discussed the use of one-step residuals in estimating the covariance matrix. In particular we point out that one-step residuals lead to a biased estimate of the covariance matrix where some correlation are zeros by definition (see Figure C.1). In addition, Tables C.4, C.5 and C.6 show the Frobenius norm, CRPS, and ES skill scores as explained in the paper to investigate the effectiveness of one-step residuals. Moreover, in Tables C.7 and C.8, we have utilized a shrinkage matrix rather than the sample covariance matrix to assess the performance of our approach.

| **Reconciliation approach** | **Generation of the base forecasts paths** | | | | | | | | |
|---|---|---|---|---|---|---|---|---|---|
| | Gaussian approach: sample covariance matrix | | | | | | | | |
| | ctjb | In-sample residuals | | | | Multi-step residuals | | | |
| | | G | B | H | HB | G | B | H | HB |
| base | 8.260 | 17.638 | 16.733 | 22.178 | 21.789 | 7.748 | 6.549 | 3.409 | 2.215 |
| ct$(bu)$ | 3.195 | 21.789 | 21.789 | **21.789** | 21.789 | 2.215 | 2.215 | **2.215** | 2.215 |
| ct$(shr_{cs}, bu_{te})$ | 3.202 | 21.942 | 21.789 | 21.942 | 21.789 | 2.224 | 2.215 | 2.224 | 2.215 |
| ct$(wlsv_{te}, bu_{cs})$ | **3.183** | 18.237 | 18.237 | 21.789 | 21.789 | **2.188** | 2.188 | **2.215** | 2.215 |
| oct$(wlsv)$ | 3.766 | 19.174 | 18.611 | 22.304 | 21.789 | 3.082 | 2.191 | 2.910 | 2.215 |
| oct$(bdshr)$ | 3.203 | 18.559 | 18.416 | 21.937 | 21.789 | 2.195 | **2.184** | 2.224 | **2.215** |
| oct$(shr)$ | 5.217 | 25.015 | 23.457 | 23.413 | **21.789** | 2.260 | 2.202 | 2.226 | 2.215 |
| oct$(bshr)$ | 5.282 | 23.772 | 23.997 | 22.146 | 21.789 | 2.720 | 2.220 | 2.756 | 2.215 |
| oct$(hshr)$ | 6.161 | **11.336** | **10.940** | 23.598 | **21.789** | 4.138 | 4.167 | 2.225 | 2.215 |
| oct$(hbshr)$ | 5.731 | 11.379 | 10.940 | 22.146 | 21.789 | 5.085 | 4.167 | 2.756 | 2.215 |
| oct$_h(shr)$ | 3.251 | 20.965 | 19.992 | 22.079 | **21.789** | 2.260 | 2.202 | 2.226 | 2.215 |
| oct$_h(bshr)$ | 3.602 | 21.306 | 21.022 | 22.146 | 21.789 | 2.720 | 2.220 | 2.756 | 2.215 |
| oct$_h(hshr)$ | 4.869 | 11.405 | 10.940 | 22.037 | 21.789 | 4.138 | 4.167 | 2.225 | 2.215 |

**Table C.4:** *Frobenius norm between the true and the estimated covariance matrix for different reconciliation approaches and different techniques for simulating the base forecasts. Entries in bold represent the lowest value for each column, while the blue entry represent the global minimum. The reconciliation approaches are described in Table 2.*

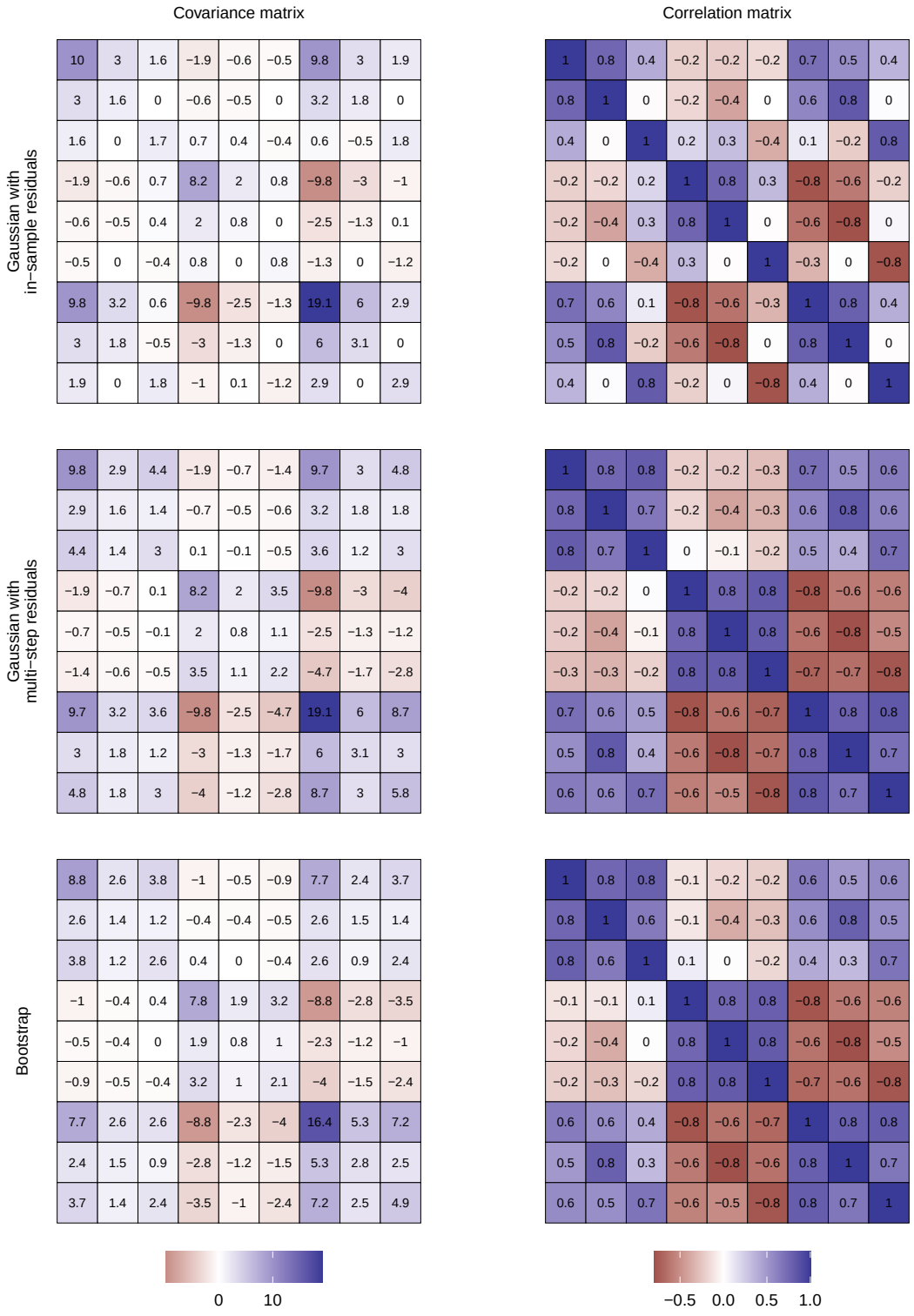


**Figure C.1:** *Comparison of estimated covariance and correlation matrices (first simulation) for base forecasts using a parametric Gaussian (with one-step residuals) approach. The true covariance and correlation matrices are shown in Figure 7.*

| Reconciliation approach | Generation of the base forecasts paths | | | | | | | | |
|---|---|---|---|---|---|---|---|---|---|
| | | Gaussian approach: sample covariance matrix | | | | | | | |
| | ctjb | In-sample residuals | | | | Multi-step residuals | | | |
| | | G | B | H | HB | G | B | H | HB |
| | | | | $\forall k \in \{2,1\}$ | | | | | |
| base | 1.000 | 1.008 | 1.009 | 1.044 | 1.047 | 0.998 | 0.999 | 1.002 | 1.004 |
| ct($bu$) | 0.901 | 0.930 | 0.929 | 0.929 | 0.929 | 0.900 | 0.900 | 0.900 | 0.900 |
| ct($shr_{cs}, bu_{te}$) | **0.901** | **0.929** | 0.928 | **0.929** | **0.928** | **0.900** | **0.899** | **0.900** | **0.900** |
| ct($wlsv_{te}, bu_{cs}$) | 0.910 | 0.930 | 0.929 | 0.939 | 0.939 | 0.916 | 0.916 | 0.916 | 0.917 |
| oct($wlsv$) | 0.922 | 0.942 | 0.944 | 0.951 | 0.953 | 0.930 | 0.930 | 0.930 | 0.931 |
| oct($bdshr$) | 0.910 | 0.930 | 0.930 | 0.939 | 0.938 | 0.916 | 0.915 | 0.916 | 0.916 |
| oct($shr$) | 0.941 | 0.999 | 0.985 | 0.983 | 0.973 | 0.903 | 0.902 | 0.902 | 0.903 |
| oct($bshr$) | 0.951 | 0.995 | 1.000 | 0.983 | 0.986 | 0.922 | 0.922 | 0.921 | 0.922 |
| oct($hshr$) | 0.987 | 0.995 | 0.993 | 1.039 | 1.026 | 0.972 | 0.972 | 0.974 | 0.975 |
| oct($hbshr$) | 0.987 | 0.995 | 0.996 | 1.024 | 1.028 | 0.985 | 0.985 | 0.987 | 0.989 |
| oct$_h$($shr$) | 0.904 | 0.929 | **0.928** | 0.932 | 0.932 | 0.903 | 0.902 | 0.902 | 0.903 |
| oct$_h$($bshr$) | 0.923 | 0.948 | 0.952 | 0.951 | 0.954 | 0.922 | 0.922 | 0.921 | 0.922 |
| oct$_h$($hshr$) | 0.974 | 0.982 | 0.982 | 1.012 | 1.012 | 0.972 | 0.972 | 0.974 | 0.975 |
| | | | | $k = 1$ | | | | | |
| base | 1.000 | 1.017 | 1.019 | 1.017 | 1.019 | 0.998 | 0.999 | 0.999 | 1.000 |
| ct($bu$) | 0.978 | 0.994 | 0.994 | 0.994 | 0.994 | 0.976 | 0.976 | 0.977 | 0.977 |
| ct($shr_{cs}, bu_{te}$) | **0.977** | **0.993** | **0.993** | **0.994** | **0.993** | **0.976** | **0.976** | **0.976** | **0.976** |
| ct($wlsv_{te}, bu_{cs}$) | 0.986 | 1.002 | 1.002 | 1.003 | 1.003 | 0.993 | 0.993 | 0.993 | 0.993 |
| oct($wlsv$) | 0.998 | 1.014 | 1.015 | 1.015 | 1.016 | 1.006 | 1.006 | 1.007 | 1.007 |
| oct($bdshr$) | 0.986 | 1.002 | 1.002 | 1.003 | 1.003 | 0.992 | 0.992 | 0.993 | 0.993 |
| oct($shr$) | 1.037 | 1.082 | 1.067 | 1.064 | 1.056 | 0.979 | 0.978 | 0.979 | 0.979 |
| oct($bshr$) | 1.041 | 1.071 | 1.074 | 1.060 | 1.062 | 0.998 | 0.998 | 0.998 | 0.998 |
| oct($hshr$) | 1.080 | 1.090 | 1.091 | 1.119 | 1.105 | 1.050 | 1.050 | 1.053 | 1.053 |
| oct($hbshr$) | 1.065 | 1.080 | 1.081 | 1.088 | 1.090 | 1.063 | 1.064 | 1.066 | 1.068 |
| oct$_h$($shr$) | 0.980 | 0.996 | 0.995 | 0.996 | 0.996 | 0.979 | 0.978 | 0.979 | 0.979 |
| oct$_h$($bshr$) | 0.999 | 1.016 | 1.018 | 1.016 | 1.018 | 0.998 | 0.998 | 0.998 | 0.998 |
| oct$_h$($hshr$) | 1.052 | 1.067 | 1.066 | 1.074 | 1.075 | 1.050 | 1.050 | 1.053 | 1.053 |
| | | | | $k = 2$ | | | | | |
| base | 1.000 | 0.998 | 0.999 | 1.071 | 1.075 | 0.998 | 0.999 | 1.005 | 1.008 |
| ct($bu$) | 0.831 | 0.869 | 0.869 | 0.869 | 0.869 | 0.830 | 0.829 | 0.829 | 0.830 |
| ct($shr_{cs}, bu_{te}$) | **0.830** | 0.869 | 0.868 | **0.868** | **0.868** | **0.830** | **0.829** | **0.829** | **0.830** |
| ct($wlsv_{te}, bu_{cs}$) | 0.840 | **0.863** | **0.862** | 0.879 | 0.878 | 0.846 | 0.844 | 0.845 | 0.846 |
| oct($wlsv$) | 0.851 | 0.875 | 0.877 | 0.891 | 0.893 | 0.859 | 0.859 | 0.859 | 0.861 |
| oct($bdshr$) | 0.839 | 0.863 | 0.863 | 0.879 | 0.878 | 0.845 | 0.844 | 0.845 | 0.846 |
| oct($shr$) | 0.854 | 0.922 | 0.909 | 0.908 | 0.897 | 0.833 | 0.831 | 0.832 | 0.832 |
| oct($bshr$) | 0.869 | 0.925 | 0.931 | 0.911 | 0.915 | 0.851 | 0.851 | 0.851 | 0.852 |
| oct($hshr$) | 0.901 | 0.908 | 0.904 | 0.966 | 0.952 | 0.900 | 0.899 | 0.901 | 0.902 |
| oct($hbshr$) | 0.915 | 0.917 | 0.919 | 0.964 | 0.969 | 0.913 | 0.913 | 0.914 | 0.917 |
| oct$_h$($shr$) | 0.834 | 0.868 | 0.865 | 0.872 | 0.872 | 0.833 | 0.831 | 0.832 | 0.832 |
| oct$_h$($bshr$) | 0.852 | 0.886 | 0.890 | 0.890 | 0.894 | 0.851 | 0.851 | 0.851 | 0.852 |
| oct$_h$($hshr$) | 0.902 | 0.904 | 0.904 | 0.953 | 0.952 | 0.900 | 0.899 | 0.901 | 0.902 |

**Table C.5:** *Simulation experiment.* $\overline{RelCRPS}$ *defined in Section 5. Approaches performing worse than the benchmark (bootstrap base forecasts, ctjb) are highlighted in red, the best for each column is marked in bold, and the overall lowest value is highlighted in blue. The reconciliation approaches are described in Table 2.*

| Reconciliation approach | Generation of the base forecasts paths | | | | | | | | |
|---|---|---|---|---|---|---|---|---|---|
| | | Gaussian approach: sample covariance matrix | | | | | | | |
| | ctjb | In-sample residuals | | | | Multi-step residuals | | | |
| | | G | B | H | HB | G | B | H | HB |
| | | | | $\forall k \in \{2,1\}$ | | | | | |
| base | 1.000 | 1.005 | 1.009 | 1.039 | 1.046 | 0.996 | 0.999 | 1.000 | 1.004 |
| ct($bu$) | 0.897 | 0.924 | 0.923 | 0.924 | 0.923 | 0.895 | 0.896 | 0.897 | **0.895** |
| ct($shr_{cs}, bu_{te}$) | **0.896** | 0.924 | 0.923 | **0.923** | **0.922** | **0.895** | **0.895** | **0.896** | 0.896 |
| ct($wlsv_{te}, bu_{cs}$) | 0.906 | 0.924 | 0.923 | 0.933 | 0.932 | 0.912 | 0.911 | 0.910 | 0.912 |
| oct($wlsv$) | 0.916 | 0.935 | 0.937 | 0.944 | 0.945 | 0.923 | 0.923 | 0.923 | 0.924 |
| oct($bdshr$) | 0.906 | **0.923** | 0.923 | 0.932 | 0.932 | 0.910 | 0.910 | 0.911 | 0.912 |
| oct($shr$) | 0.938 | 0.993 | 0.980 | 0.977 | 0.969 | 0.898 | 0.898 | 0.898 | 0.897 |
| oct($bshr$) | 0.947 | 0.990 | 0.995 | 0.979 | 0.981 | 0.915 | 0.915 | 0.915 | 0.915 |
| oct($hshr$) | 0.978 | 0.987 | 0.985 | 1.027 | 1.016 | 0.963 | 0.964 | 0.966 | 0.967 |
| oct($hbshr$) | 0.977 | 0.986 | 0.985 | 1.012 | 1.016 | 0.974 | 0.976 | 0.977 | 0.978 |
| oct$_h$($shr$) | 0.900 | 0.923 | **0.922** | 0.926 | 0.925 | 0.898 | 0.898 | 0.897 | 0.898 |
| oct$_h$($bshr$) | 0.916 | 0.940 | 0.943 | 0.942 | 0.945 | 0.914 | 0.916 | 0.915 | 0.916 |
| oct$_h$($hshr$) | 0.967 | 0.974 | 0.974 | 1.002 | 1.002 | 0.964 | 0.964 | 0.966 | 0.967 |
| | | | | $k = 1$ | | | | | |
| base | 1.000 | 1.014 | 1.020 | 1.015 | 1.019 | 0.997 | 1.000 | 0.997 | 1.000 |
| ct($bu$) | 0.969 | 0.985 | 0.983 | 0.985 | 0.984 | **0.967** | **0.967** | 0.968 | **0.968** |
| ct($shr_{cs}, bu_{te}$) | **0.968** | **0.984** | **0.983** | **0.984** | **0.983** | 0.968 | 0.967 | **0.968** | 0.968 |
| ct($wlsv_{te}, bu_{cs}$) | 0.977 | 0.991 | 0.991 | 0.992 | 0.992 | 0.984 | 0.983 | 0.981 | 0.984 |
| oct($wlsv$) | 0.989 | 1.002 | 1.004 | 1.003 | 1.004 | 0.994 | 0.995 | 0.995 | 0.997 |
| oct($bdshr$) | 0.977 | 0.989 | 0.991 | 0.992 | 0.992 | 0.981 | 0.982 | 0.983 | 0.985 |
| oct($shr$) | 1.028 | 1.070 | 1.056 | 1.053 | 1.046 | 0.969 | 0.969 | 0.970 | 0.969 |
| oct($bshr$) | 1.034 | 1.061 | 1.065 | 1.051 | 1.053 | 0.985 | 0.987 | 0.986 | 0.987 |
| oct($hshr$) | 1.066 | 1.075 | 1.076 | 1.099 | 1.090 | 1.037 | 1.037 | 1.039 | 1.039 |
| oct($hbshr$) | 1.050 | 1.065 | 1.065 | 1.070 | 1.073 | 1.048 | 1.049 | 1.049 | 1.052 |
| oct$_h$($shr$) | 0.971 | 0.985 | 0.985 | 0.986 | 0.986 | 0.969 | 0.969 | 0.969 | 0.969 |
| oct$_h$($bshr$) | 0.987 | 1.002 | 1.005 | 1.002 | 1.005 | 0.986 | 0.987 | 0.987 | 0.988 |
| oct$_h$($hshr$) | 1.040 | 1.053 | 1.053 | 1.059 | 1.058 | 1.036 | 1.036 | 1.040 | 1.040 |
| | | | | $k = 2$ | | | | | |
| base | 1.000 | 0.997 | 0.999 | 1.063 | 1.073 | 0.996 | 0.998 | 1.003 | 1.008 |
| ct($bu$) | 0.831 | 0.867 | 0.867 | 0.867 | 0.867 | 0.829 | 0.829 | 0.830 | **0.828** |
| ct($shr_{cs}, bu_{te}$) | **0.829** | 0.867 | 0.866 | **0.866** | **0.865** | **0.828** | **0.829** | **0.829** | 0.829 |
| ct($wlsv_{te}, bu_{cs}$) | 0.839 | **0.860** | **0.860** | 0.877 | 0.876 | 0.844 | 0.844 | 0.844 | 0.845 |
| oct($wlsv$) | 0.849 | 0.872 | 0.875 | 0.887 | 0.890 | 0.858 | 0.856 | 0.856 | 0.857 |
| oct($bdshr$) | 0.839 | 0.861 | 0.861 | 0.876 | 0.875 | 0.845 | 0.843 | 0.845 | 0.844 |
| oct($shr$) | 0.856 | 0.921 | 0.909 | 0.907 | 0.898 | 0.832 | 0.831 | 0.832 | 0.831 |
| oct($bshr$) | 0.868 | 0.924 | 0.930 | 0.911 | 0.915 | 0.849 | 0.848 | 0.849 | 0.848 |
| oct($hshr$) | 0.897 | 0.905 | 0.901 | 0.959 | 0.947 | 0.895 | 0.896 | 0.898 | 0.899 |
| oct($hbshr$) | 0.910 | 0.912 | 0.912 | 0.957 | 0.961 | 0.906 | 0.909 | 0.909 | 0.910 |
| oct$_h$($shr$) | 0.835 | 0.865 | 0.862 | 0.870 | 0.868 | 0.833 | 0.833 | 0.831 | 0.832 |
| oct$_h$($bshr$) | 0.850 | 0.881 | 0.885 | 0.886 | 0.889 | 0.847 | 0.849 | 0.849 | 0.850 |
| oct$_h$($hshr$) | 0.900 | 0.902 | 0.901 | 0.947 | 0.948 | 0.897 | 0.896 | 0.897 | 0.899 |

**Table C.6:** *Simulation experiment. ES ratio indices defined in Section 5. Approaches performing worse than the benchmark (bootstrap base forecasts, ctjb) are highlighted in red, the best for each column is marked in bold, and the overall lowest value is highlighted in blue. The reconciliation approaches are described in Table 2.*

| Reconciliation approach | Generation of the base forecasts paths | | | | | | | | |
|---|---|---|---|---|---|---|---|---|---|
| | | Gaussian approach: shrinkage covariance matrix | | | | | | | |
| | ctjb | In-sample residuals | | | | Multi-step residuals | | | |
| | | G | B | H | HB | G | B | H | HB |
| | | | | $\forall k \in \{2,1\}$ | | | | | |
| base | 1.007 | 1.009 | 1.044 | 1.046 | 0.997 | 0.999 | 1.002 | 1.003 | 1.000 |
| ct($bu$) | 0.929 | 0.929 | 0.929 | 0.929 | 0.899 | 0.900 | 0.900 | 0.900 | 0.901 |
| ct($shr_{cs}, bu_{te}$) | **0.929** | 0.928 | **0.929** | **0.928** | **0.899** | **0.899** | **0.900** | **0.900** | **0.901** |
| ct($wlsv_{te}, bu_{cs}$) | 0.930 | 0.930 | 0.939 | 0.938 | 0.915 | 0.916 | 0.917 | 0.916 | 0.910 |
| oct($wlsv$) | 0.943 | 0.944 | 0.951 | 0.952 | 0.929 | 0.930 | 0.931 | 0.930 | 0.922 |
| oct($bdshr$) | 0.930 | 0.930 | 0.938 | 0.938 | 0.915 | 0.916 | 0.916 | 0.916 | 0.910 |
| oct($shr$) | 0.994 | 0.982 | 0.980 | 0.973 | 0.902 | 0.902 | 0.903 | 0.902 | 0.941 |
| oct($bshr$) | 0.995 | 0.998 | 0.983 | 0.986 | 0.921 | 0.922 | 0.922 | 0.922 | 0.951 |
| oct($hshr$) | 0.994 | 0.994 | 1.035 | 1.025 | 0.971 | 0.972 | 0.974 | 0.974 | 0.987 |
| oct($hbshr$) | 0.995 | 0.997 | 1.025 | 1.027 | 0.984 | 0.986 | 0.988 | 0.988 | 0.987 |
| oct$_h$($shr$) | 0.929 | **0.928** | 0.932 | 0.932 | 0.902 | 0.902 | 0.903 | 0.902 | 0.904 |
| oct$_h$($bshr$) | 0.948 | 0.951 | 0.951 | 0.953 | 0.921 | 0.922 | 0.922 | 0.922 | 0.923 |
| oct$_h$($hshr$) | 0.982 | 0.982 | 1.011 | 1.011 | 0.971 | 0.972 | 0.974 | 0.974 | 0.974 |
| | | | | $k = 1$ | | | | | |
| base | 1.017 | 1.019 | 1.017 | 1.019 | 0.998 | 0.999 | 0.999 | 0.999 | 1.000 |
| ct($bu$) | 0.994 | 0.994 | 0.994 | 0.994 | 0.976 | 0.976 | 0.977 | 0.976 | 0.978 |
| ct($shr_{cs}, bu_{te}$) | **0.993** | **0.993** | **0.993** | **0.993** | **0.975** | **0.976** | **0.976** | **0.976** | **0.977** |
| ct($wlsv_{te}, bu_{cs}$) | 1.002 | 1.002 | 1.003 | 1.003 | 0.992 | 0.993 | 0.993 | 0.993 | 0.986 |
| oct($wlsv$) | 1.015 | 1.015 | 1.015 | 1.016 | 1.005 | 1.007 | 1.007 | 1.007 | 0.998 |
| oct($bdshr$) | 1.002 | 1.002 | 1.003 | 1.002 | 0.992 | 0.992 | 0.993 | 0.992 | 0.986 |
| oct($shr$) | 1.076 | 1.065 | 1.061 | 1.056 | 0.978 | 0.978 | 0.979 | 0.978 | 1.037 |
| oct($bshr$) | 1.070 | 1.072 | 1.060 | 1.062 | 0.997 | 0.998 | 0.998 | 0.998 | 1.041 |
| oct($hshr$) | 1.090 | 1.092 | 1.114 | 1.105 | 1.049 | 1.050 | 1.053 | 1.052 | 1.080 |
| oct($hbshr$) | 1.080 | 1.081 | 1.089 | 1.090 | 1.062 | 1.064 | 1.066 | 1.066 | 1.065 |
| oct$_h$($shr$) | 0.996 | 0.995 | 0.996 | 0.996 | 0.978 | 0.978 | 0.979 | 0.978 | 0.980 |
| oct$_h$($bshr$) | 1.016 | 1.018 | 1.016 | 1.018 | 0.997 | 0.998 | 0.998 | 0.998 | 0.999 |
| oct$_h$($hshr$) | 1.066 | 1.067 | 1.075 | 1.075 | 1.049 | 1.050 | 1.053 | 1.052 | 1.052 |
| | | | | $k = 2$ | | | | | |
| base | 0.997 | 0.999 | 1.071 | 1.074 | 0.997 | 0.999 | 1.005 | 1.008 | 1.000 |
| ct($bu$) | 0.869 | 0.868 | 0.868 | 0.868 | 0.829 | 0.829 | 0.830 | 0.830 | 0.831 |
| ct($shr_{cs}, bu_{te}$) | 0.868 | 0.867 | **0.868** | **0.867** | **0.829** | **0.829** | **0.830** | **0.829** | **0.830** |
| ct($wlsv_{te}, bu_{cs}$) | **0.863** | **0.862** | 0.878 | 0.878 | 0.845 | 0.845 | 0.846 | 0.846 | 0.840 |
| oct($wlsv$) | 0.876 | 0.877 | 0.891 | 0.892 | 0.859 | 0.860 | 0.860 | 0.860 | 0.851 |
| oct($bdshr$) | 0.863 | 0.863 | 0.878 | 0.877 | 0.844 | 0.845 | 0.846 | 0.845 | 0.839 |
| oct($shr$) | 0.918 | 0.906 | 0.906 | 0.897 | 0.832 | 0.832 | 0.833 | 0.832 | 0.854 |
| oct($bshr$) | 0.924 | 0.928 | 0.911 | 0.915 | 0.850 | 0.851 | 0.852 | 0.851 | 0.869 |
| oct($hshr$) | 0.907 | 0.905 | 0.962 | 0.951 | 0.898 | 0.899 | 0.902 | 0.902 | 0.901 |
| oct($hbshr$) | 0.917 | 0.919 | 0.964 | 0.968 | 0.912 | 0.913 | 0.915 | 0.916 | 0.915 |
| oct$_h$($shr$) | 0.867 | 0.864 | 0.872 | 0.871 | 0.832 | 0.832 | 0.833 | 0.832 | 0.834 |
| oct$_h$($bshr$) | 0.886 | 0.890 | 0.890 | 0.893 | 0.850 | 0.851 | 0.852 | 0.851 | 0.852 |
| oct$_h$($hshr$) | 0.904 | 0.905 | 0.952 | 0.952 | 0.898 | 0.899 | 0.902 | 0.902 | 0.902 |

**Table C.7:** *Simulation experiment.* $\overline{RelCRPS}$ *defined in Section 5. Approaches performing worse than the benchmark (bootstrap base forecasts, ctjb) are highlighted in red, the best for each column is marked in bold, and the overall lowest value is highlighted in blue. The reconciliation approaches are described in Table 2.*

| Reconciliation approach | Generation of the base forecasts paths | | | | | | | | |
|---|---|---|---|---|---|---|---|---|---|
| | | Gaussian approach: shrinkage covariance matrix | | | | | | | |
| | ctjb | In-sample residuals | | | | Multi-step residuals | | | |
| | | G | B | H | HB | G | B | H | HB |
| | | | | $\forall k \in \{2,1\}$ | | | | | |
| base | 1.005 | 1.008 | 1.039 | 1.045 | 0.996 | 0.999 | 1.000 | 1.003 | 1.000 |
| ct($bu$) | **0.923** | 0.923 | 0.923 | 0.923 | **0.895** | 0.896 | 0.897 | 0.897 | 0.897 |
| ct($shr_{cs}, bu_{te}$) | 0.923 | 0.922 | **0.922** | **0.922** | 0.896 | **0.895** | **0.895** | **0.895** | **0.896** |
| ct($wlsv_{te}, bu_{cs}$) | 0.924 | 0.924 | 0.932 | 0.932 | 0.910 | 0.911 | 0.911 | 0.911 | 0.906 |
| oct($wlsv$) | 0.935 | 0.937 | 0.944 | 0.945 | 0.922 | 0.924 | 0.923 | 0.923 | 0.916 |
| oct($bdshr$) | 0.924 | 0.924 | 0.932 | 0.931 | 0.909 | 0.911 | 0.911 | 0.910 | 0.906 |
| oct($shr$) | 0.989 | 0.978 | 0.975 | 0.968 | 0.897 | 0.898 | 0.898 | 0.898 | 0.938 |
| oct($bshr$) | 0.990 | 0.993 | 0.978 | 0.981 | 0.915 | 0.915 | 0.915 | 0.915 | 0.947 |
| oct($hshr$) | 0.986 | 0.985 | 1.024 | 1.015 | 0.963 | 0.964 | 0.966 | 0.967 | 0.978 |
| oct($hbshr$) | 0.985 | 0.986 | 1.012 | 1.015 | 0.973 | 0.976 | 0.977 | 0.978 | 0.977 |
| oct$_h$($shr$) | 0.923 | **0.922** | 0.925 | 0.925 | 0.897 | 0.898 | 0.898 | 0.898 | 0.900 |
| oct$_h$($bshr$) | 0.941 | 0.943 | 0.942 | 0.945 | 0.913 | 0.915 | 0.915 | 0.915 | 0.916 |
| oct$_h$($hshr$) | 0.974 | 0.975 | 1.001 | 1.001 | 0.964 | 0.964 | 0.966 | 0.966 | 0.967 |
| | | | | $k = 1$ | | | | | |
| base | 1.014 | 1.018 | 1.015 | 1.019 | 0.997 | 0.999 | 0.997 | 0.998 | 1.000 |
| ct($bu$) | 0.983 | 0.984 | 0.984 | 0.984 | 0.967 | 0.967 | 0.969 | 0.969 | 0.969 |
| ct($shr_{cs}, bu_{te}$) | **0.983** | **0.982** | **0.982** | **0.983** | **0.966** | **0.967** | **0.966** | **0.966** | **0.968** |
| ct($wlsv_{te}, bu_{cs}$) | 0.991 | 0.992 | 0.993 | 0.992 | 0.983 | 0.983 | 0.983 | 0.983 | 0.977 |
| oct($wlsv$) | 1.002 | 1.004 | 1.004 | 1.004 | 0.994 | 0.995 | 0.994 | 0.996 | 0.989 |
| oct($bdshr$) | 0.990 | 0.991 | 0.992 | 0.991 | 0.981 | 0.983 | 0.984 | 0.982 | 0.977 |
| oct($shr$) | 1.065 | 1.054 | 1.051 | 1.045 | 0.969 | 0.970 | 0.970 | 0.969 | 1.028 |
| oct($bshr$) | 1.061 | 1.063 | 1.050 | 1.052 | 0.986 | 0.986 | 0.987 | 0.985 | 1.034 |
| oct($hshr$) | 1.076 | 1.077 | 1.095 | 1.088 | 1.036 | 1.036 | 1.040 | 1.038 | 1.066 |
| oct($hbshr$) | 1.064 | 1.065 | 1.071 | 1.073 | 1.047 | 1.048 | 1.050 | 1.050 | 1.050 |
| oct$_h$($shr$) | 0.984 | 0.985 | 0.986 | 0.986 | 0.969 | 0.969 | 0.969 | 0.968 | 0.971 |
| oct$_h$($bshr$) | 1.003 | 1.005 | 1.003 | 1.005 | 0.985 | 0.987 | 0.987 | 0.986 | 0.987 |
| oct$_h$($hshr$) | 1.054 | 1.054 | 1.059 | 1.059 | 1.036 | 1.037 | 1.038 | 1.039 | 1.040 |
| | | | | $k = 2$ | | | | | |
| base | 0.996 | 0.998 | 1.064 | 1.073 | 0.995 | 0.999 | 1.003 | 1.007 | 1.000 |
| ct($bu$) | 0.867 | 0.866 | 0.867 | 0.866 | **0.829** | 0.829 | 0.830 | 0.830 | 0.831 |
| ct($shr_{cs}, bu_{te}$) | 0.867 | 0.866 | **0.866** | **0.866** | 0.830 | **0.829** | **0.830** | **0.830** | **0.829** |
| ct($wlsv_{te}, bu_{cs}$) | **0.861** | **0.861** | 0.875 | 0.875 | 0.843 | 0.845 | 0.845 | 0.845 | 0.839 |
| oct($wlsv$) | 0.873 | 0.874 | 0.888 | 0.889 | 0.856 | 0.857 | 0.857 | 0.856 | 0.849 |
| oct($bdshr$) | 0.862 | 0.861 | 0.876 | 0.874 | 0.843 | 0.844 | 0.844 | 0.844 | 0.839 |
| oct($shr$) | 0.918 | 0.907 | 0.905 | 0.898 | 0.831 | 0.832 | 0.832 | 0.832 | 0.856 |
| oct($bshr$) | 0.924 | 0.928 | 0.911 | 0.915 | 0.849 | 0.849 | 0.849 | 0.849 | 0.868 |
| oct($hshr$) | 0.904 | 0.901 | 0.957 | 0.946 | 0.895 | 0.896 | 0.898 | 0.900 | 0.897 |
| oct($hbshr$) | 0.912 | 0.913 | 0.956 | 0.961 | 0.905 | 0.909 | 0.909 | 0.911 | 0.910 |
| oct$_h$($shr$) | 0.866 | 0.863 | 0.869 | 0.869 | 0.830 | 0.831 | 0.832 | 0.832 | 0.835 |
| oct$_h$($bshr$) | 0.882 | 0.886 | 0.886 | 0.889 | 0.846 | 0.848 | 0.849 | 0.848 | 0.850 |
| oct$_h$($hshr$) | 0.901 | 0.902 | 0.947 | 0.946 | 0.896 | 0.896 | 0.898 | 0.899 | 0.900 |

**Table C.8:** *Simulation experiment. ES ratio indices defined in Section 5. Approaches performing worse than the benchmark (bootstrap base forecasts, ctjb) are highlighted in red, the best for each column is marked in bold, and the overall lowest value is highlighted in blue. The reconciliation approaches are described in Table 2.*

# D Forecast reconciliation of the Australian GDP dataset

## D.1 The dataset

Athanasopoulos et al. (2020) proposed using state-of-the-art forecast reconciliation methods to improve the accuracy of macroeconomic forecasts and facilitate aligned decision-making. In their empirical analysis, they applied cross-sectional forecast reconciliation to 95 Australian QNA time series that represent the Gross Domestic Product (GDP) calculated using both the income and expenditure approaches. These two approaches correspond to two distinct hierarchical structures, with GDP at the top and 15 lower-level aggregates in the income approach, and GDP as the top-level aggregate in a hierarchy of 79 time series in the expenditure approach (for more information, see Athanasopoulos et al. 2020, pp. 702–705 and figures 21.4–21.7). Bisaglia et al. (2020) showed how to obtain a "one-number" forecast where the GDP reconciled forecasts are coherent for both the expenditure and income sides. Di Fonzo & Girolimetto (2022*c*), Girolimetto & Di Fonzo (2023*b*) extended the one number forecasts idea to obtain fully reconciled probabilistic forecasts, and Di Fonzo & Girolimetto (2023*a*) computed cross-temporally reconciled point forecasts.

## D.2 One-step residuals and shrinkage covariance matrix

| Reconciliation approach | Generation of the base forecasts paths | | | | | | | | | |
|---|---|---|---|---|---|---|---|---|---|---|
| | ctjb | Gaussian approach* | | | | ctjb | Gaussian approach* | | | |
| | | $G_h$ | $H_h$ | $G_{oh}$ | $H_{oh}$ | | $G_h$ | $H_h$ | $G_{oh}$ | $H_{oh}$ |
| | $\forall k \in \{4,2,1\}$ | | | | | $k=1$ | | | | |
| base | 1.000 | 0.979 | 0.995 | 0.968 | 0.976 | 1.000 | 0.988 | 0.988 | 0.971 | 0.971 |
| ct($shr_{cs}, bu_{te}$) | 0.937 | 0.956 | 0.956 | 0.976 | 0.976 | 0.992 | 1.008 | 1.008 | 1.029 | 1.029 |
| ct($wls_{cs}, bu_{te}$) | 0.930 | 0.917 | 0.917 | 0.898 | 0.898 | 0.986 | 0.974 | 0.975 | 0.956 | 0.956 |
| oct($wlsv$) | 0.926 | 0.919 | 0.920 | 0.900 | 0.900 | 0.984 | 0.981 | 0.979 | 0.959 | 0.959 |
| oct($bdshr$) | 0.940 | 0.965 | 0.945 | 0.992 | 0.957 | 0.997 | 1.019 | 1.003 | 1.044 | 1.018 |
| oct($shr$) | 0.944 | 1.020 | 0.940 | 1.094 | 0.988 | 1.015 | 1.095 | 1.010 | 1.160 | 1.059 |
| oct($hshr$) | 0.988 | 0.972 | 1.002 | 0.974 | 1.001 | 1.048 | 1.037 | 1.060 | 1.034 | 1.061 |
| $oct_o$($wlsv$) | **0.926** | **0.911** | **0.912** | **0.896** | **0.895** | **0.984** | **0.971** | **0.970** | **0.954** | **0.954** |
| $oct_o$($bdshr$) | 0.978 | 0.964 | 0.946 | 0.952 | 0.930 | 1.034 | 1.016 | 1.003 | 1.005 | 0.989 |
| $oct_o$($shr$) | 0.950 | 0.946 | 0.922 | 0.925 | 0.903 | 1.014 | 1.003 | 0.985 | 0.987 | 0.968 |
| $oct_o$($hshr$) | 0.989 | 0.966 | 0.984 | 0.954 | 0.965 | 1.047 | 1.028 | 1.038 | 1.012 | 1.023 |
| $oct_{oh}$($shr$) | 1.102 | 1.059 | 1.001 | 1.094 | 0.988 | 1.172 | 1.109 | 1.066 | 1.160 | 1.059 |
| $oct_{oh}$($hshr$) | 1.006 | 0.983 | 1.009 | 0.974 | 1.001 | 1.068 | 1.046 | 1.059 | 1.034 | 1.061 |
| | $k=2$ | | | | | $k=4$ | | | | |
| base | 1.000 | 0.984 | 0.993 | 0.968 | 0.976 | 1.000 | 0.966 | 1.004 | 0.964 | 0.981 |
| ct($shr_{cs}, bu_{te}$) | 0.949 | 0.966 | 0.966 | 0.987 | 0.987 | 0.874 | 0.896 | 0.896 | 0.914 | 0.914 |
| ct($wls_{cs}, bu_{te}$) | 0.942 | 0.928 | 0.928 | 0.909 | 0.909 | 0.866 | 0.853 | 0.853 | 0.834 | 0.834 |
| oct($wlsv$) | 0.938 | 0.929 | 0.931 | 0.911 | 0.911 | 0.860 | 0.853 | 0.855 | 0.835 | 0.834 |
| oct($bdshr$) | 0.953 | 0.976 | 0.956 | 1.003 | 0.969 | 0.874 | 0.904 | 0.880 | 0.931 | 0.889 |
| oct($shr$) | 0.955 | 1.031 | 0.951 | 1.113 | 1.002 | 0.866 | 0.940 | 0.864 | 1.015 | 0.909 |
| oct($hshr$) | 1.001 | 0.985 | 1.014 | 0.987 | 1.016 | 0.919 | 0.900 | 0.935 | 0.904 | 0.931 |
| $oct_o$($wlsv$) | **0.938** | **0.921** | **0.923** | **0.907** | **0.906** | **0.860** | **0.847** | **0.848** | **0.832** | **0.830** |
| $oct_o$($bdshr$) | 0.991 | 0.974 | 0.957 | 0.964 | 0.942 | 0.914 | 0.905 | 0.883 | 0.892 | 0.865 |
| $oct_o$($shr$) | 0.965 | 0.958 | 0.934 | 0.938 | 0.916 | 0.877 | 0.882 | 0.852 | 0.854 | 0.831 |
| $oct_o$($hshr$) | 1.002 | 0.979 | 0.996 | 0.967 | 0.978 | 0.922 | 0.898 | 0.923 | 0.888 | 0.898 |
| $oct_{oh}$($shr$) | 1.120 | 1.069 | 1.013 | 1.113 | 1.002 | 1.020 | 1.002 | 0.928 | 1.015 | 0.909 |
| $oct_{oh}$($hshr$) | 1.021 | 0.996 | 1.021 | 0.987 | 1.016 | 0.934 | 0.912 | 0.951 | 0.904 | 0.931 |

*The Gaussian method employs a sample covariance matrix:
$G_h$ and $H_h$ use multi-step residuals and $G_{oh}$ and $H_{oh}$ use overlapping and multi-step residuals.

**Table D.1:** *$\overline{RelCRPS}$ indices defined in Section 5 for the Australian QNA dataset. Approaches performing worse than the benchmark (bootstrap base forecasts, ctjb) are highlighted in red, the best for each column is marked in bold, and the overall lowest value is highlighted in blue. The reconciliation approaches are described in Table 2.*

| Reconciliation approach | Generation of the base forecasts paths | | | | | | | | | |
|---|---|---|---|---|---|---|---|---|---|---|
| | ctjb | Gaussian approach* | | | | ctjb | Gaussian approach* | | | |
| | | $G_h$ | $H_h$ | $G_{oh}$ | $H_{oh}$ | | $G_h$ | $H_h$ | $G_{oh}$ | $H_{oh}$ |
| | $\forall k \in \{4,2,1\}$ | | | | | $k=1$ | | | | |
| base | 1.000 | 0.970 | 0.988 | 0.960 | 0.970 | 1.000 | 0.977 | 0.977 | 0.965 | 0.965 |
| ct($shr_{cs}, bu_{te}$) | 0.897 | 0.944 | 0.944 | 0.973 | 0.973 | 0.964 | 1.001 | 1.001 | 1.033 | 1.033 |
| ct($wls_{cs}, bu_{te}$) | **0.886** | 0.880 | 0.880 | **0.860** | 0.860 | **0.954** | **0.944** | 0.945 | **0.928** | **0.928** |
| oct($wlsv$) | 0.890 | 0.890 | 0.894 | 0.872 | 0.872 | 0.958 | 0.957 | 0.957 | 0.938 | 0.939 |
| oct($bdshr$) | 0.905 | 0.956 | 0.934 | 0.992 | 0.954 | 0.972 | 1.014 | 0.994 | 1.048 | 1.018 |
| oct($shr$) | 0.895 | 0.979 | 0.895 | 1.053 | 0.944 | 0.973 | 1.060 | 0.969 | 1.121 | 1.015 |
| oct($hshr$) | 0.951 | 0.940 | 0.973 | 0.959 | 0.992 | 1.017 | 1.010 | 1.034 | 1.023 | 1.055 |
| oct$_o$($wlsv$) | 0.891 | **0.879** | 0.881 | 0.864 | 0.864 | 0.958 | 0.945 | 0.945 | 0.931 | 0.931 |
| oct$_o$($bdshr$) | 0.940 | 0.928 | 0.910 | 0.918 | 0.895 | 1.004 | 0.986 | 0.971 | 0.980 | 0.961 |
| oct$_o$($shr$) | 0.900 | 0.899 | **0.876** | 0.878 | **0.858** | 0.973 | 0.963 | **0.944** | 0.949 | 0.930 |
| oct$_o$($hshr$) | 0.956 | 0.936 | 0.955 | 0.922 | 0.936 | 1.021 | 1.004 | 1.012 | 0.987 | 1.000 |
| oct$_{oh}$($shr$) | 1.059 | 1.015 | 0.956 | 1.053 | 0.945 | 1.130 | 1.063 | 1.019 | 1.121 | 1.016 |
| oct$_{oh}$($hshr$) | 0.986 | 0.968 | 0.999 | 0.959 | 0.992 | 1.053 | 1.034 | 1.049 | 1.024 | 1.055 |
| | $k=2$ | | | | | $k=4$ | | | | |
| base | 1.000 | 0.972 | 0.985 | 0.959 | 0.969 | 1.000 | 0.959 | 1.000 | 0.957 | 0.976 |
| ct($shr_{cs}, bu_{te}$) | 0.915 | 0.961 | 0.960 | 0.991 | 0.991 | 0.818 | 0.874 | 0.874 | 0.899 | 0.900 |
| ct($wls_{cs}, bu_{te}$) | **0.904** | 0.896 | **0.896** | **0.877** | **0.877** | **0.807** | 0.805 | 0.805 | **0.782** | 0.783 |
| oct($wlsv$) | 0.909 | 0.907 | 0.912 | 0.889 | 0.889 | 0.811 | 0.813 | 0.819 | 0.794 | 0.794 |
| oct($bdshr$) | 0.925 | 0.976 | 0.953 | 1.013 | 0.974 | 0.825 | 0.883 | 0.860 | 0.920 | 0.876 |
| oct($shr$) | 0.913 | 1.000 | 0.914 | 1.076 | 0.963 | 0.807 | 0.885 | 0.808 | 0.967 | 0.861 |
| oct($hshr$) | 0.973 | 0.960 | 0.993 | 0.978 | 1.014 | 0.871 | 0.856 | 0.897 | 0.881 | 0.913 |
| oct$_o$($wlsv$) | 0.908 | **0.895** | 0.898 | 0.881 | 0.882 | 0.812 | **0.802** | 0.806 | 0.786 | 0.786 |
| oct$_o$($bdshr$) | 0.960 | 0.947 | 0.929 | 0.938 | 0.915 | 0.860 | 0.856 | 0.836 | 0.841 | 0.816 |
| oct$_o$($shr$) | 0.921 | 0.919 | 0.896 | 0.898 | 0.878 | 0.814 | 0.821 | **0.796** | 0.794 | **0.775** |
| oct$_o$($hshr$) | 0.977 | 0.956 | 0.976 | 0.942 | 0.957 | 0.876 | 0.854 | 0.882 | 0.844 | 0.856 |
| oct$_{oh}$($shr$) | 1.082 | 1.029 | 0.973 | 1.076 | 0.963 | 0.971 | 0.954 | 0.882 | 0.967 | 0.861 |
| oct$_{oh}$($hshr$) | 1.007 | 0.988 | 1.017 | 0.979 | 1.014 | 0.904 | 0.888 | 0.934 | 0.881 | 0.913 |

*The Gaussian method employs a sample covariance matrix:
$G_h$ and $H_h$ use multi-step residuals and $G_{oh}$ and $H_{oh}$ use overlapping and multi-step residuals.

**Table D.2:** *ES ratio indices defined in Section 5 for the Australian QNA dataset. Approaches performing worse than the benchmark (bootstrap base forecasts, ctjb) are highlighted in red, the best for each column is marked in bold, and the overall lowest value is highlighted in blue. The reconciliation approaches are described in Table 2.*

| Reconciliation approach | Generation of the base forecasts paths | | | | | | | | | |
|---|---|---|---|---|---|---|---|---|---|---|
| | ctjb | Gaussian approach* | | | | ctjb | Gaussian approach* | | | |
| | | $G_h$ | $H_h$ | $G_{oh}$ | $H_{oh}$ | | $G_h$ | $H_h$ | $G_{oh}$ | $H_{oh}$ |
| | $\forall k \in \{4,2,1\}$ | | | | | $k=1$ | | | | |
| base | 1.000 | 0.979 | 1.011 | 0.968 | 0.987 | 1.000 | 0.988 | 0.988 | 0.971 | 0.971 |
| ct($shr_{cs}, bu_{te}$) | 0.937 | 0.960 | 0.961 | 0.962 | 0.960 | 0.992 | 1.001 | 1.001 | 1.004 | 1.000 |
| ct($wls_{cs}, bu_{te}$) | 0.930 | **0.951** | 0.953 | **0.911** | 0.915 | 0.986 | 0.997 | 0.998 | **0.964** | 0.967 |
| oct($wlsv$) | 0.926 | 0.972 | 0.957 | 0.918 | 0.917 | 0.984 | 1.010 | 1.003 | 0.971 | 0.970 |
| oct($bdshr$) | 0.940 | 0.986 | 0.966 | 0.981 | 0.956 | 0.997 | 1.015 | 1.006 | 1.016 | 1.000 |
| oct($shr$) | 0.944 | 0.999 | 0.962 | 1.051 | 0.995 | 1.015 | 1.047 | 1.021 | 1.105 | 1.058 |
| oct($hshr$) | 0.988 | 1.000 | 1.021 | 0.979 | 1.002 | 1.048 | 1.045 | 1.066 | 1.034 | 1.053 |
| oct$_o$($wlsv$) | **0.926** | 0.961 | 0.948 | 0.914 | **0.912** | **0.984** | 1.000 | 0.993 | 0.966 | **0.965** |
| oct$_o$($bdshr$) | 0.978 | 0.956 | 0.949 | 0.949 | 0.934 | 1.034 | **0.984** | **0.983** | 0.988 | 0.977 |
| oct$_o$($shr$) | 0.950 | 0.957 | **0.946** | 0.933 | 0.917 | 1.014 | 0.998 | 0.995 | 0.986 | 0.974 |
| oct$_o$($hshr$) | 0.989 | 0.997 | 1.013 | 0.967 | 0.982 | 1.047 | 1.039 | 1.054 | 1.019 | 1.032 |
| oct$_{oh}$($shr$) | 1.102 | 1.010 | 1.006 | 1.051 | 0.995 | 1.172 | 1.059 | 1.063 | 1.105 | 1.058 |
| oct$_{oh}$($hshr$) | 1.006 | 0.989 | 1.004 | 0.979 | 1.002 | 1.068 | 1.037 | 1.050 | 1.034 | 1.053 |
| | | | $k=2$ | | | | | $k=4$ | | |
| base | 1.000 | 0.984 | 1.009 | 0.968 | 0.987 | 1.000 | 0.966 | 1.037 | 0.964 | 1.002 |
| ct($shr_{cs}, bu_{te}$) | 0.949 | 0.972 | 0.972 | 0.974 | 0.971 | 0.874 | 0.910 | 0.911 | 0.910 | 0.910 |
| ct($wls_{cs}, bu_{te}$) | 0.942 | **0.962** | 0.964 | **0.923** | 0.927 | 0.866 | **0.897** | 0.900 | **0.851** | 0.855 |
| oct($wlsv$) | 0.938 | 0.988 | 0.968 | 0.931 | 0.929 | 0.860 | 0.921 | 0.903 | 0.856 | 0.856 |
| oct($bdshr$) | 0.953 | 1.004 | 0.979 | 0.996 | 0.970 | 0.874 | 0.942 | 0.914 | 0.932 | 0.900 |
| oct($shr$) | 0.955 | 1.016 | 0.973 | 1.070 | 1.010 | 0.866 | 0.937 | 0.895 | 0.981 | 0.922 |
| oct($hshr$) | 1.001 | 1.015 | 1.034 | 0.993 | 1.017 | 0.919 | 0.942 | 0.965 | 0.913 | 0.937 |
| oct$_o$($wlsv$) | **0.938** | 0.976 | **0.959** | 0.927 | **0.925** | **0.860** | 0.910 | 0.894 | 0.853 | 0.852 |
| oct$_o$($bdshr$) | 0.991 | 0.970 | 0.963 | 0.963 | 0.948 | 0.914 | 0.917 | 0.905 | 0.899 | 0.880 |
| oct$_o$($shr$) | 0.965 | 0.973 | 0.959 | 0.948 | 0.931 | 0.877 | 0.903 | **0.886** | 0.868 | **0.850** |
| oct$_o$($hshr$) | 1.002 | 1.013 | 1.026 | 0.980 | 0.996 | 0.922 | 0.943 | 0.962 | 0.905 | 0.921 |
| oct$_{oh}$($shr$) | 1.120 | 1.026 | 1.019 | 1.070 | 1.010 | 1.020 | 0.947 | 0.939 | 0.981 | 0.922 |
| oct$_{oh}$($hshr$) | 1.021 | 1.005 | 1.017 | 0.993 | 1.017 | 0.934 | 0.929 | 0.946 | 0.913 | 0.937 |

*The Gaussian method employs a shrinkage covariance matrix:
$G_h$ and $H_h$ use multi-step residuals and $G_{oh}$ and $H_{oh}$ use overlapping and multi-step residuals.

**Table D.3:** *$\overline{RelCRPS}$ indices defined in Section 5 for the Australian QNA dataset. Approaches performing worse than the benchmark (bootstrap base forecasts, ctjb) are highlighted in red, the best for each column is marked in bold, and the overall lowest value is highlighted in blue. The reconciliation approaches are described in Table 2.*

| Reconciliation approach | Generation of the base forecasts paths | | | | | | | | | |
|---|---|---|---|---|---|---|---|---|---|---|
| | ctjb | Gaussian approach* | | | | ctjb | Gaussian approach* | | | |
| | | $G_h$ | $H_h$ | $G_{oh}$ | $H_{oh}$ | | $G_h$ | $H_h$ | $G_{oh}$ | $H_{oh}$ |
| | $\forall k \in \{4,2,1\}$ | | | | | $k=1$ | | | | |
| base | 1.000 | 0.967 | 1.002 | 0.957 | 0.980 | 1.000 | 0.973 | 0.973 | 0.961 | 0.962 |
| ct($shr_{cs}, bu_{te}$) | 0.897 | 0.968 | 0.969 | 0.963 | 0.962 | 0.964 | 1.012 | 1.012 | 1.009 | 1.004 |
| ct($wls_{cs}, bu_{te}$) | **0.886** | 0.939 | 0.944 | **0.882** | 0.888 | **0.954** | 0.994 | 0.998 | **0.947** | 0.952 |
| oct($wlsv$) | 0.890 | 0.966 | 0.959 | 0.897 | 0.901 | 0.958 | 1.017 | 1.012 | 0.960 | 0.965 |
| oct($bdshr$) | 0.905 | 0.997 | 0.981 | 0.986 | 0.960 | 0.972 | 1.031 | 1.021 | 1.024 | 1.005 |
| oct($shr$) | 0.895 | 0.979 | 0.945 | 1.021 | 0.962 | 0.973 | 1.041 | 1.011 | 1.083 | 1.028 |
| oct($hshr$) | 0.951 | 0.997 | 1.023 | 0.973 | 1.005 | 1.017 | 1.051 | 1.073 | 1.034 | 1.063 |
| oct$_o$($wlsv$) | 0.891 | 0.950 | 0.945 | 0.889 | 0.892 | 0.958 | 1.002 | 0.997 | 0.953 | 0.956 |
| oct$_o$($bdshr$) | 0.940 | 0.935 | 0.933 | 0.922 | 0.909 | 1.004 | **0.965** | **0.964** | 0.969 | 0.959 |
| oct$_o$($shr$) | 0.900 | **0.935** | **0.928** | 0.895 | **0.884** | 0.973 | 0.984 | 0.982 | 0.960 | **0.950** |
| oct$_o$($hshr$) | 0.956 | 0.997 | 1.015 | 0.945 | 0.965 | 1.021 | 1.049 | 1.062 | 1.007 | 1.024 |
| oct$_{oh}$($shr$) | 1.059 | 0.981 | 0.983 | 1.021 | 0.962 | 1.130 | 1.034 | 1.041 | 1.083 | 1.029 |
| oct$_{oh}$($hshr$) | 0.986 | 0.996 | 1.014 | 0.973 | 1.005 | 1.053 | 1.050 | 1.064 | 1.034 | 1.063 |
| | $k=2$ | | | | | $k=4$ | | | | |
| base | 1.000 | 0.970 | 0.999 | 0.955 | 0.980 | 1.000 | 0.958 | 1.033 | 0.953 | 1.000 |
| ct($shr_{cs}, bu_{te}$) | 0.915 | 0.987 | 0.988 | 0.983 | 0.982 | 0.818 | 0.909 | 0.910 | 0.902 | 0.902 |
| ct($wls_{cs}, bu_{te}$) | **0.904** | **0.958** | 0.962 | **0.900** | 0.906 | **0.807** | 0.871 | 0.876 | **0.805** | 0.812 |
| oct($wlsv$) | 0.909 | 0.988 | 0.979 | 0.916 | 0.920 | 0.811 | 0.896 | 0.891 | 0.820 | 0.825 |
| oct($bdshr$) | 0.925 | 1.024 | 1.005 | 1.010 | 0.984 | 0.825 | 0.938 | 0.919 | 0.926 | 0.895 |
| oct($shr$) | 0.913 | 1.006 | 0.967 | 1.045 | 0.982 | 0.807 | 0.898 | 0.864 | 0.940 | 0.881 |
| oct($hshr$) | 0.973 | 1.020 | 1.046 | 0.994 | 1.028 | 0.871 | 0.924 | 0.954 | 0.897 | 0.929 |
| oct$_o$($wlsv$) | 0.908 | 0.972 | 0.964 | 0.908 | 0.911 | 0.812 | 0.882 | 0.876 | 0.812 | 0.816 |
| oct$_o$($bdshr$) | 0.960 | 0.959 | 0.957 | 0.945 | 0.932 | 0.860 | 0.884 | 0.879 | 0.857 | 0.841 |
| oct$_o$($shr$) | 0.921 | 0.958 | **0.950** | 0.917 | **0.905** | 0.814 | **0.867** | **0.857** | 0.815 | **0.803** |
| oct$_o$($hshr$) | 0.977 | 1.021 | 1.038 | 0.966 | 0.987 | 0.876 | 0.926 | 0.949 | 0.868 | 0.889 |
| oct$_{oh}$($shr$) | 1.082 | 1.002 | 1.003 | 1.045 | 0.982 | 0.971 | 0.910 | 0.911 | 0.941 | 0.882 |
| oct$_{oh}$($hshr$) | 1.007 | 1.017 | 1.036 | 0.994 | 1.028 | 0.904 | 0.924 | 0.947 | 0.896 | 0.929 |

*The Gaussian method employs a shrinkage covariance matrix:
$G_h$ and $H_h$ use multi-step residuals and $G_{oh}$ and $H_{oh}$ use overlapping and multi-step residuals.

**Table D.4:** *ES ratio indices defined in Section 5 for the Australian QNA dataset. Approaches performing worse than the benchmark (bootstrap base forecasts, ctjb) are highlighted in red, the best for each column is marked in bold, and the overall lowest value is highlighted in blue. The reconciliation approaches are described in Table 2.*

# E Australian Tourism Demand dataset

**Table E.1:** *Geographic divisions of Australia in States, Zones e Regions. Zones formed by a single region are highlighted in italics and not numbered.*

| Series | Name | Label | Series | Name | Label |
|---|---|---|---|---|---|
| *Total* | | | *continues Regions* | | |
| 1 | Australia | Total | 49 | Gippsland | BCB |
| *States* | | | 50 | Phillip Island | BCC |
| 2 | New South Wales (NSW) | A | 51 | Central Murray | BDA |
| 3 | Victoria (VIC) | B | 52 | Goulburn | BDB |
| 4 | Queensland (QLD) | C | 53 | High Country | BDC |
| 5 | South Australia (SA) | D | 54 | Melbourne East | BDD |
| 6 | Western Australia (WA) | E | 55 | Upper Yarra | BDE |
| 7 | Tasmania (TAS) | F | 56 | MurrayEast | BDF |
| 8 | Northern Territory (NT) | G | 57 | Mallee | BEA |
| *Zones* | | | 58 | Wimmera | BEB |
| 9 | Metro NSW | AA | 59 | Western Grampians | BEC |
| 10 | Nth Coast NSW | AB | 60 | Bendigo Loddon | BED |
| | *Sth Coast NSW* | *AC* | 61 | Macedon | BEE |
| 11 | Sth NSW | AD | 62 | Spa Country | BEF |
| 12 | Nth NSW | AE | 63 | Ballarat | BEG |
| | *ACT* | *AF* | 64 | Central Highlands | BEG |
| 13 | Metro VIC | BA | 65 | Gold Coast | CAA |
| | *West Coast VIC* | *BB* | 66 | Brisbane | CAB |
| 14 | East Coast VIC | BC | 67 | Sunshine Coast | CAC |
| 15 | Nth East VIC | BD | 68 | Central Queensland | CBA |
| 16 | Nth West VIC | BE | 69 | Bundaberg | CBB |
| 17 | Metro QLD | CA | 70 | Fraser Coast | CBC |
| 18 | Central Coast QLD | CB | 71 | Mackay | CBD |
| 19 | Nth Coast QLD | CC | 72 | Whitsundays | CCA |
| 20 | Inland QLD | CD | 73 | Northern | CCB |
| 21 | Metro SA | DA | 74 | Tropical North Queensland | CCC |
| 22 | Sth Coast SA | DB | 75 | Darling Downs | CDA |
| 23 | Inland SA | DC | 76 | Outback | CDB |
| 24 | West Coast SA | DD | 77 | Adelaide | DAA |
| 25 | West CoastWA | EA | 78 | Barossa | DAB |
| | *Nth WA* | *EB* | 79 | Adelaide Hills | DAC |
| | *SthWA* | *EC* | 80 | Limestone Coast | DBA |
| | *Sth TAS* | *FA* | 81 | Fleurieu Peninsula | DBB |
| 26 | Nth East TAS | FB | 82 | Kangaroo Island | DBC |
| 27 | Nth West TAS | FC | 83 | Murraylands | DCA |
| 28 | Nth Coast NT | GA | 84 | Riverland | DCB |
| 29 | Central NT | GB | 85 | Clare Valley | DCC |
| *Regions* | | | 86 | Flinders Range and Outback | DCD |
| 30 | Sydney | AAA | 87 | Eyre Peninsula | DDA |
| 31 | Central Coast | AAB | 88 | Yorke Peninsula | DDB |
| 32 | Hunter | ABA | 89 | Australia's Coral Coast | EAA |
| 33 | North Coast NSW | ABB | 90 | Experience Perth | EAB |
| 34 | South Coast | ACA | 91 | Australia's SouthWest | EAC |
| 35 | Snowy Mountains | ADA | 92 | Australia's North West | EBA |
| 36 | Capital Country | ADB | 93 | Australia's Golden Outback | ECA |
| 37 | The Murray | ADC | 94 | Hobart and the South | FAA |
| 38 | Riverina | ADD | 95 | East Coast | FBA |
| 39 | Central NSW | AEA | 96 | Launceston, Tamar and the North | FBB |
| 40 | New England North West | AEB | 97 | North West | FCA |
| 41 | Outback NSW | AEC | 98 | WildernessWest | FCB |
| 42 | Blue Mountains | AED | 99 | Darwin | GAA |
| 43 | Canberra | AFA | 100 | Kakadu Arnhem | GAB |
| 44 | Melbourne | BAA | 101 | Katherine Daly | GAC |
| 45 | Peninsula | BAB | 102 | Barkly | GBA |
| 46 | Geelong | BAC | 103 | Lasseter | GBB |
| 47 | Western | BBA | 104 | Alice Springs | GBC |
| 48 | Lakes | BCA | 105 | MacDonnell | GBD |

Source: Wickramasuriya et al. (2019), Di Fonzo & Girolimetto (2022*b*)

### E.1 Dealing with negative reconciled forecasts

One issue in working with time series data is the presence of negative values, which can cause difficulties for certain types of models or analyses. For the base forecasts, using the bootstrap approach produces forecasts naturally non negative (ETS model with the log-transformation), while this is not true for the Gaussian approach. In this case, any negative forecast is set equal to zero. For the cross-temporal reconciliation, Di Fonzo & Girolimetto (2022*a*, 2023*b*) propose two solutions: either a state-of-the-art numerical optimization procedure (`osqp`, Stellato et al. 2020, 2022), or a simple heuristic strategy called set-negative-to-zero (sntz). With sntz, any negative high frequency bottom time series reconciled forecasts are set to zero, and then a cross-temporal reconciliation bottom-up is used to obtain the complete set of fully coherent forecasts. Di Fonzo & Girolimetto (2023*b*) found that both methods produce similar quality forecasts, but the optimization method required much more time and computational effort compared to the sntz heuristic. To reduce computational demands, we used the less time-intensive heuristic approach for reconciliation.

## E.2 Tables for all the temporal aggregation orders

| Reconciliation approach | Generation of the base forecasts paths | | | | | | | | | |
|---|---|---|---|---|---|---|---|---|---|---|
| | ctjb | Gaussian approach* | | | | ctjb | Gaussian approach* | | | |
| | | G | B | H | HB | | G | B | H | HB |
| | | $\forall k \in \{12,6,4,3,2,1\}$ | | | | | | $k=1$ | | |
| base | 1.000 | 0.971 | 0.971 | 0.973 | 0.973 | 1.000 | 0.972 | 0.972 | 0.972 | 0.972 |
| ct($bu$) | 1.321 | 1.011 | 1.011 | 1.011 | 1.011 | 1.077 | 0.983 | 0.982 | 0.982 | 0.982 |
| ct($shr_{cs}, bu_{te}$) | 1.057 | 0.974 | 0.969 | 0.974 | 0.969 | 0.976 | 0.963 | 0.962 | 0.963 | 0.962 |
| ct($wlsv_{te}, bu_{cs}$) | 1.062 | 0.974 | 0.974 | 0.972 | 0.972 | 0.976 | 0.965 | 0.965 | 0.966 | 0.966 |
| oct($ols$) | 0.989 | 0.989 | 0.989 | 0.987 | 0.987 | 0.982 | 0.986 | 0.988 | 0.986 | 0.989 |
| oct($struc$) | 0.982 | 0.962 | 0.961 | 0.961 | 0.959 | 0.970 | 0.963 | 0.963 | 0.963 | 0.963 |
| oct($wlsv$) | 0.987 | 0.959 | 0.959 | 0.958 | 0.957 | 0.952 | 0.957 | 0.957 | 0.957 | 0.957 |
| oct($bdshr$) | 0.975 | **0.956** | **0.953** | **0.952** | **0.951** | **0.949** | **0.955** | **0.953** | **0.954** | **0.954** |
| oct$_h$($bshr$) | 0.994 | 1.018 | 1.020 | 1.016 | 1.019 | 0.988 | 1.007 | 1.013 | 1.006 | 1.012 |
| oct$_h$($hshr$) | **0.969** | 0.993 | 0.993 | 0.990 | 0.991 | 0.953 | 0.977 | 0.977 | 0.979 | 0.979 |
| oct$_h$($shr$) | 1.007 | 0.980 | 0.972 | 0.970 | 0.970 | 1.000 | 0.986 | 0.977 | 0.976 | 0.974 |
| | | | $k=2$ | | | | | $k=3$ | | |
| base | 1.000 | 0.970 | 0.969 | 0.970 | 0.971 | 1.000 | 0.971 | 0.971 | 0.972 | 0.973 |
| ct($bu$) | 1.189 | 0.999 | 0.999 | 0.999 | 0.999 | 1.273 | 1.010 | 1.010 | 1.010 | 1.010 |
| ct($shr_{cs}, bu_{te}$) | 1.015 | 0.972 | 0.970 | 0.972 | 0.970 | 1.041 | 0.977 | 0.974 | 0.977 | 0.974 |
| ct($wlsv_{te}, bu_{cs}$) | 1.016 | 0.971 | 0.971 | 0.970 | 0.970 | 1.046 | 0.976 | 0.976 | 0.974 | 0.974 |
| oct($ols$) | 0.992 | 0.991 | 0.991 | 0.990 | 0.991 | 0.994 | 0.992 | 0.993 | 0.991 | 0.992 |
| oct($struc$) | 0.982 | 0.966 | 0.965 | 0.965 | 0.965 | 0.986 | 0.967 | 0.966 | 0.966 | 0.965 |
| oct($wlsv$) | 0.972 | 0.961 | 0.960 | 0.960 | 0.960 | 0.983 | 0.963 | 0.962 | 0.962 | 0.962 |
| oct($bdshr$) | **0.964** | **0.958** | **0.957** | **0.956** | **0.956** | 0.972 | **0.960** | **0.958** | **0.957** | **0.957** |
| oct$_h$($bshr$) | 0.997 | 1.015 | 1.018 | 1.013 | 1.017 | 0.999 | 1.021 | 1.022 | 1.018 | 1.022 |
| oct$_h$($hshr$) | 0.965 | 0.987 | 0.987 | 0.986 | 0.987 | **0.971** | 0.994 | 0.994 | 0.992 | 0.993 |
| oct$_h$($shr$) | 1.005 | 0.986 | 0.978 | 0.976 | 0.975 | 1.009 | 0.986 | 0.978 | 0.976 | 0.976 |
| | | | $k=4$ | | | | | $k=6$ | | |
| base | 1.000 | 0.973 | 0.973 | 0.974 | 0.975 | 1.000 | 0.976 | 0.976 | 0.978 | 0.978 |
| ct($bu$) | 1.340 | 1.016 | 1.015 | 1.015 | 1.015 | 1.450 | 1.023 | 1.023 | 1.023 | 1.023 |
| ct($shr_{cs}, bu_{te}$) | 1.061 | 0.978 | 0.973 | 0.978 | 0.973 | 1.094 | 0.978 | 0.972 | 0.978 | 0.972 |
| ct($wlsv_{te}, bu_{cs}$) | 1.068 | 0.977 | 0.977 | 0.974 | 0.974 | 1.103 | 0.977 | 0.977 | 0.974 | 0.974 |
| oct($ols$) | 0.993 | 0.991 | 0.992 | 0.990 | 0.990 | 0.989 | 0.989 | 0.989 | 0.987 | 0.986 |
| oct($struc$) | 0.986 | 0.965 | 0.964 | 0.964 | 0.963 | 0.986 | 0.961 | 0.960 | 0.959 | 0.957 |
| oct($wlsv$) | 0.990 | 0.962 | 0.961 | 0.961 | 0.960 | 1.001 | 0.960 | 0.959 | 0.958 | 0.957 |
| oct($bdshr$) | 0.977 | **0.959** | **0.956** | **0.955** | **0.954** | 0.985 | **0.956** | **0.953** | **0.950** | **0.948** |
| oct$_h$($bshr$) | 0.997 | 1.022 | 1.022 | 1.019 | 1.022 | 0.994 | 1.022 | 1.022 | 1.020 | 1.022 |
| oct$_h$($hshr$) | **0.973** | 0.996 | 0.997 | 0.994 | 0.995 | **0.976** | 1.000 | 1.001 | 0.996 | 0.997 |
| oct$_h$($shr$) | 1.009 | 0.984 | 0.976 | 0.973 | 0.973 | 1.010 | 0.978 | 0.970 | 0.967 | 0.967 |
| | | | $k=12$ | | | | | | | |
| base | 1.000 | 0.968 | 0.967 | 0.969 | 0.969 | | | | | |
| ct($bu$) | 1.675 | 1.038 | 1.037 | 1.037 | 1.038 | | | | | |
| ct($shr_{cs}, bu_{te}$) | 1.163 | 0.977 | 0.965 | 0.977 | 0.965 | | | | | |
| ct($wlsv_{te}, bu_{cs}$) | 1.174 | 0.978 | 0.978 | 0.971 | 0.971 | | | | | |
| oct($ols$) | 0.982 | 0.982 | 0.983 | 0.980 | 0.975 | | | | | |
| oct($struc$) | 0.982 | 0.951 | 0.949 | 0.947 | 0.943 | | | | | |
| oct($wlsv$) | 1.025 | 0.954 | 0.953 | 0.949 | 0.947 | | | | | |
| oct($bdshr$) | 1.002 | **0.950** | **0.944** | **0.939** | **0.935** | | | | | |
| oct$_h$($bshr$) | 0.987 | 1.024 | 1.021 | 1.021 | 1.019 | | | | | |
| oct$_h$($hshr$) | **0.978** | 1.003 | 1.005 | 0.996 | 0.997 | | | | | |
| oct$_h$($shr$) | 1.010 | 0.963 | 0.956 | 0.952 | 0.952 | | | | | |

*The Gaussian method employs a sample covariance matrix and includes four techniques (G, B, H, HB) with multi-step residuals.

**Table E.2:** *$\overline{RelCRPS}$ defined in Section 5 for the Australian Tourism Demand dataset. Approaches performing worse than the benchmark (bootstrap base forecasts, ctjb) are highlighted in red, the best for each column is marked in bold, and the overall lowest value is highlighted in blue. The reconciliation approaches are described in Table 2.*

| Reconciliation approach | Generation of the base forecasts paths | | | | | | | | | |
|---|---|---|---|---|---|---|---|---|---|---|
| | ctjb | Gaussian approach* | | | | ctjb | Gaussian approach* | | | |
| | | G | B | H | HB | | G | B | H | HB |
| | | $\forall k \in \{12,6,4,3,2,1\}$ | | | | | | $k=1$ | | |
| base | 1.000 | 0.956 | 0.955 | 0.958 | 0.951 | 1.000 | 0.952 | 0.950 | 0.952 | 0.950 |
| ct($bu$) | 2.427 | 0.983 | 0.983 | 0.983 | 0.983 | 1.759 | 0.982 | 0.982 | 0.982 | 0.982 |
| ct($shr_{cs}, bu_{te}$) | 1.243 | 0.886 | 0.879 | 0.886 | 0.879 | 1.098 | 0.929 | 0.928 | 0.930 | 0.927 |
| ct($wlsv_{te}, bu_{cs}$) | 1.499 | 0.977 | 0.977 | 0.971 | 0.972 | 1.241 | 0.975 | 0.975 | 0.973 | 0.974 |
| oct($ols$) | 0.955 | 0.893 | 0.891 | 0.893 | 0.888 | 0.975 | 0.937 | 0.936 | 0.936 | 0.935 |
| oct($struc$) | 1.085 | 0.917 | 0.915 | 0.916 | 0.912 | 1.027 | 0.943 | 0.942 | 0.943 | 0.942 |
| oct($wlsv$) | 1.132 | 0.933 | 0.929 | 0.931 | 0.927 | 1.050 | 0.951 | 0.949 | 0.950 | 0.949 |
| oct($bdshr$) | 1.047 | 0.904 | 0.897 | 0.897 | 0.891 | 1.009 | 0.936 | 0.933 | 0.934 | 0.931 |
| oct$_h$($bshr$) | **0.931** | **0.867** | **0.866** | **0.863** | **0.860** | **0.965** | **0.927** | 0.927 | 0.925 | 0.923 |
| oct$_h$($hshr$) | 1.081 | 0.935 | 0.931 | 0.935 | 0.927 | 1.028 | 0.952 | 0.951 | 0.952 | 0.950 |
| oct$_h$($shr$) | 1.068 | 0.899 | 0.878 | 0.875 | 0.864 | 1.023 | 0.935 | **0.923** | **0.921** | **0.916** |
| | | | $k=2$ | | | | | $k=3$ | | |
| base | 1.000 | 0.958 | 0.954 | 0.956 | 0.953 | 1.000 | 0.961 | 0.958 | 0.960 | 0.955 |
| ct($bu$) | 2.176 | 1.001 | 1.001 | 1.001 | 1.001 | 2.428 | 0.998 | 0.997 | 0.997 | 0.997 |
| ct($shr_{cs}, bu_{te}$) | 1.192 | 0.927 | 0.921 | 0.927 | 0.921 | 1.245 | 0.911 | 0.904 | 0.911 | 0.904 |
| ct($wlsv_{te}, bu_{cs}$) | 1.400 | 0.992 | 0.992 | 0.988 | 0.988 | 1.500 | 0.991 | 0.991 | 0.986 | 0.987 |
| oct($ols$) | 0.985 | 0.935 | 0.932 | 0.934 | 0.930 | 0.976 | 0.918 | 0.915 | 0.917 | 0.912 |
| oct($struc$) | 1.075 | 0.949 | 0.947 | 0.948 | 0.944 | 1.096 | 0.939 | 0.936 | 0.938 | 0.933 |
| oct($wlsv$) | 1.110 | 0.960 | 0.958 | 0.958 | 0.955 | 1.142 | 0.953 | 0.949 | 0.951 | 0.946 |
| oct($bdshr$) | 1.045 | 0.938 | 0.933 | 0.933 | 0.929 | 1.060 | 0.926 | 0.920 | 0.921 | 0.915 |
| oct$_h$($bshr$) | **0.967** | **0.917** | **0.916** | 0.913 | 0.908 | **0.954** | **0.895** | **0.895** | **0.892** | **0.887** |
| oct$_h$($hshr$) | 1.073 | 0.962 | 0.959 | 0.963 | 0.956 | 1.093 | 0.955 | 0.951 | 0.956 | 0.949 |
| oct$_h$($shr$) | 1.064 | 0.933 | 0.916 | **0.913** | **0.904** | 1.082 | 0.923 | 0.903 | 0.900 | 0.890 |
| | | | $k=4$ | | | | | $k=6$ | | |
| base | 1.000 | 0.960 | 0.960 | 0.962 | 0.956 | 1.000 | 0.961 | 0.959 | 0.964 | 0.956 |
| ct($bu$) | 2.585 | 0.996 | 0.996 | 0.995 | 0.996 | 2.849 | 1.004 | 1.003 | 1.003 | 1.004 |
| ct($shr_{cs}, bu_{te}$) | 1.277 | 0.898 | 0.890 | 0.899 | 0.891 | 1.339 | 0.882 | 0.873 | 0.883 | 0.874 |
| ct($wlsv_{te}, bu_{cs}$) | 1.559 | 0.990 | 0.990 | 0.984 | 0.985 | 1.662 | 0.997 | 0.997 | 0.991 | 0.992 |
| oct($ols$) | 0.966 | 0.905 | 0.902 | 0.904 | 0.899 | 0.962 | 0.889 | 0.887 | 0.890 | 0.885 |
| oct($struc$) | 1.106 | 0.930 | 0.927 | 0.928 | 0.924 | 1.132 | 0.923 | 0.919 | 0.922 | 0.916 |
| oct($wlsv$) | 1.157 | 0.947 | 0.943 | 0.945 | 0.939 | 1.192 | 0.942 | 0.937 | 0.941 | 0.934 |
| oct($bdshr$) | 1.065 | 0.917 | 0.909 | 0.910 | 0.903 | 1.084 | 0.907 | 0.897 | 0.898 | 0.890 |
| oct$_h$($bshr$) | **0.943** | **0.879** | **0.878** | **0.876** | **0.871** | **0.932** | **0.856** | **0.855** | **0.851** | **0.848** |
| oct$_h$($hshr$) | 1.101 | 0.949 | 0.944 | 0.949 | 0.941 | 1.126 | 0.945 | 0.939 | 0.945 | 0.936 |
| oct$_h$($shr$) | 1.089 | 0.915 | 0.893 | 0.890 | 0.878 | 1.107 | 0.899 | 0.875 | 0.871 | 0.858 |
| | | | $k=12$ | | | | | | | |
| base | 1.000 | 0.942 | 0.947 | 0.951 | 0.937 | | | | | |
| ct($bu$) | 2.990 | 0.922 | 0.921 | 0.923 | 0.923 | | | | | |
| ct($shr_{cs}, bu_{te}$) | 1.326 | 0.779 | 0.767 | 0.777 | 0.766 | | | | | |
| ct($wlsv_{te}, bu_{cs}$) | 1.679 | 0.917 | 0.917 | 0.906 | 0.908 | | | | | |
| oct($ols$) | 0.872 | 0.783 | 0.784 | 0.783 | 0.779 | | | | | |
| oct($struc$) | 1.077 | 0.826 | 0.822 | 0.823 | 0.818 | | | | | |
| oct($wlsv$) | 1.149 | 0.851 | 0.845 | 0.847 | 0.840 | | | | | |
| oct($bdshr$) | 1.021 | 0.808 | 0.796 | 0.796 | 0.787 | | | | | |
| oct$_h$($bshr$) | **0.833** | **0.741** | **0.741** | **0.737** | **0.735** | | | | | |
| oct$_h$($hshr$) | 1.066 | 0.851 | 0.846 | 0.848 | 0.838 | | | | | |
| oct$_h$($shr$) | 1.043 | 0.797 | 0.768 | 0.764 | 0.750 | | | | | |

*The Gaussian method employs a sample covariance matrix and includes four techniques (G, B, H, HB) with multi-step residuals.

**Table E.3:** *ES ratio indices defined in Section 5 for the Australian Tourism Demand dataset. Approaches performing worse than the benchmark (bootstrap base forecasts, ctjb) are highlighted in red, the best for each column is marked in bold, and the overall lowest value is highlighted in blue. The reconciliation approaches are described in Table 2.*

| Reconciliation approach | Generation of the base forecasts paths | | | | | | | | | |
|---|---|---|---|---|---|---|---|---|---|---|
| | ctjb | Gaussian approach* | | | | ctjb | Gaussian approach* | | | |
| | | G | B | H | HB | | G | B | H | HB |
| | | $\forall k \in \{12,6,4,3,2,1\}$ | | | | | | $k=1$ | | |
| base | 1.000 | **0.971** | 0.972 | **0.971** | 0.972 | 1.000 | **0.972** | 0.971 | 0.972 | 0.971 |
| ct($bu$) | 1.321 | 1.017 | 1.018 | 1.017 | 1.017 | 1.077 | 0.983 | 0.983 | 0.983 | 0.983 |
| ct($shr_{cs}, bu_{te}$) | 1.057 | 1.013 | **0.971** | 1.013 | 0.971 | 0.976 | 0.987 | **0.961** | 0.988 | 0.961 |
| ct($wlsv_{te}, bu_{cs}$) | 1.062 | 1.069 | 1.070 | 0.974 | 0.974 | 0.976 | 0.986 | 0.986 | **0.965** | 0.965 |
| oct($ols$) | 0.989 | 1.163 | 1.052 | 1.139 | 0.987 | 0.982 | 1.038 | 0.992 | 1.047 | 0.987 |
| oct($struc$) | 0.982 | 1.099 | 1.039 | 1.037 | 0.960 | 0.970 | 1.007 | 0.971 | 0.999 | 0.962 |
| oct($wlsv$) | 0.987 | 1.080 | 1.041 | 0.992 | 0.958 | 0.952 | 1.004 | 0.969 | 0.978 | 0.956 |
| oct($bdshr$) | 0.975 | 1.072 | 1.032 | 0.985 | **0.950** | **0.949** | 0.999 | 0.965 | 0.975 | **0.952** |
| oct$_h$($bshr$) | 0.994 | 1.202 | 1.073 | 1.168 | 1.021 | 0.988 | 1.046 | 1.012 | 1.063 | 1.012 |
| oct$_h$($hshr$) | **0.969** | 1.066 | 1.052 | 1.008 | 0.994 | 0.953 | 0.994 | 0.972 | 0.991 | 0.979 |
| oct$_h$($shr$) | 1.007 | 1.090 | 1.046 | 1.000 | 0.970 | 1.000 | 1.035 | 0.992 | 0.998 | 0.973 |
| | | | $k=2$ | | | | | $k=3$ | | |
| base | 1.000 | **0.969** | 0.969 | **0.968** | 0.968 | 1.000 | **0.971** | **0.970** | **0.969** | 0.970 |
| ct($bu$) | 1.189 | 1.000 | 1.000 | 1.000 | 1.000 | 1.273 | 1.013 | 1.013 | 1.013 | 1.013 |
| ct($shr_{cs}, bu_{te}$) | 1.015 | 1.004 | **0.968** | 1.004 | 0.968 | 1.041 | 1.013 | 0.973 | 1.014 | 0.973 |
| ct($wlsv_{te}, bu_{cs}$) | 1.016 | 1.043 | 1.044 | 0.969 | 0.969 | 1.046 | 1.067 | 1.068 | 0.974 | 0.974 |
| oct($ols$) | 0.992 | 1.118 | 1.037 | 1.092 | 0.989 | 0.994 | 1.153 | 1.053 | 1.124 | 0.990 |
| oct($struc$) | 0.982 | 1.075 | 1.022 | 1.020 | 0.963 | 0.986 | 1.099 | 1.041 | 1.033 | 0.964 |
| oct($wlsv$) | 0.972 | 1.064 | 1.021 | 0.987 | 0.958 | 0.983 | 1.083 | 1.041 | 0.993 | 0.960 |
| oct($bdshr$) | **0.964** | 1.057 | 1.015 | 0.983 | **0.953** | 0.972 | 1.075 | 1.033 | 0.988 | **0.955** |
| oct$_h$($bshr$) | 0.997 | 1.145 | 1.059 | 1.114 | 1.016 | 0.999 | 1.190 | 1.075 | 1.151 | 1.021 |
| oct$_h$($hshr$) | 0.965 | 1.050 | 1.029 | 1.001 | 0.986 | **0.971** | 1.067 | 1.051 | 1.009 | 0.994 |
| oct$_h$($shr$) | 1.005 | 1.083 | 1.035 | 1.001 | 0.973 | 1.009 | 1.097 | 1.050 | 1.004 | 0.974 |
| | | | $k=4$ | | | | | $k=6$ | | |
| base | 1.000 | **0.973** | **0.973** | **0.971** | 0.973 | 1.000 | **0.976** | 0.977 | **0.975** | 0.977 |
| ct($bu$) | 1.340 | 1.021 | 1.021 | 1.021 | 1.021 | 1.450 | 1.032 | 1.033 | 1.032 | 1.033 |
| ct($shr_{cs}, bu_{te}$) | 1.061 | 1.018 | 0.974 | 1.018 | 0.974 | 1.094 | 1.023 | **0.974** | 1.024 | 0.974 |
| ct($wlsv_{te}, bu_{cs}$) | 1.068 | 1.087 | 1.089 | 0.976 | 0.976 | 1.103 | 1.108 | 1.110 | 0.978 | 0.978 |
| oct($ols$) | 0.993 | 1.186 | 1.068 | 1.148 | 0.989 | 0.989 | 1.223 | 1.080 | 1.184 | 0.987 |
| oct($struc$) | 0.986 | 1.120 | 1.057 | 1.042 | 0.962 | 0.986 | 1.141 | 1.071 | 1.054 | 0.959 |
| oct($wlsv$) | 0.990 | 1.100 | 1.059 | 0.996 | 0.959 | 1.001 | 1.115 | 1.076 | 0.998 | 0.958 |
| oct($bdshr$) | 0.977 | 1.091 | 1.049 | 0.989 | **0.952** | 0.985 | 1.103 | 1.064 | 0.989 | **0.949** |
| oct$_h$($bshr$) | 0.997 | 1.230 | 1.089 | 1.178 | 1.023 | 0.994 | 1.278 | 1.101 | 1.219 | 1.025 |
| oct$_h$($hshr$) | **0.973** | 1.084 | 1.071 | 1.012 | 0.996 | **0.976** | 1.097 | 1.091 | 1.017 | 1.002 |
| oct$_h$($shr$) | 1.009 | 1.108 | 1.062 | 1.003 | 0.972 | 1.010 | 1.113 | 1.070 | 1.000 | 0.968 |
| | | | $k=12$ | | | | | | | |
| base | 1.000 | **0.968** | **0.969** | **0.969** | 0.971 | | | | | |
| ct($bu$) | 1.675 | 1.056 | 1.057 | 1.057 | 1.057 | | | | | |
| ct($shr_{cs}, bu_{te}$) | 1.163 | 1.032 | 0.974 | 1.033 | 0.974 | | | | | |
| ct($wlsv_{te}, bu_{cs}$) | 1.174 | 1.128 | 1.130 | 0.982 | 0.982 | | | | | |
| oct($ols$) | 0.982 | 1.277 | 1.085 | 1.252 | 0.982 | | | | | |
| oct($struc$) | 0.982 | 1.158 | 1.074 | 1.075 | 0.950 | | | | | |
| oct($wlsv$) | 1.025 | 1.122 | 1.085 | 1.001 | 0.954 | | | | | |
| oct($bdshr$) | 1.002 | 1.110 | 1.071 | 0.989 | **0.941** | | | | | |
| oct$_h$($bshr$) | 0.987 | 1.347 | 1.107 | 1.297 | 1.031 | | | | | |
| oct$_h$($hshr$) | **0.978** | 1.106 | 1.107 | 1.021 | 1.010 | | | | | |
| oct$_h$($shr$) | 1.010 | 1.107 | 1.067 | 0.991 | 0.959 | | | | | |

*The Gaussian method employs a shrikage covariance matrix and includes four techniques (G, B, H, HB) with multi-step residuals..

**Table E.4:** *$\overline{RelCRPS}$ defined in Section 5 for the Australian Tourism Demand dataset. Approaches performing worse than the benchmark (bootstrap base forecasts, ctjb) are highlighted in red, the best for each column is marked in bold, and the overall lowest value is highlighted in blue. The reconciliation approaches are described in Table 2.*

| Reconciliation approach | Generation of the base forecasts paths | | | | | | | | | |
|---|---|---|---|---|---|---|---|---|---|---|
| | ctjb | Gaussian approach* | | | | ctjb | Gaussian approach* | | | |
| | | G | B | H | HB | | G | B | H | HB |
| | | $\forall k \in \{12,6,4,3,2,1\}$ | | | | | | $k=1$ | | |
| base | 1.000 | **0.958** | 0.984 | **0.972** | 0.992 | 1.000 | **0.954** | 0.958 | **0.954** | 0.958 |
| ct($bu$) | 2.427 | 1.040 | 1.042 | 1.040 | 1.041 | 1.759 | 1.001 | 1.002 | 1.002 | 1.002 |
| ct($shr_{cs}, bu_{te}$) | 1.243 | 0.988 | **0.913** | 0.990 | 0.913 | 1.098 | 1.011 | **0.938** | 1.013 | 0.938 |
| ct($wlsv_{te}, bu_{cs}$) | 1.499 | 1.117 | 1.120 | 1.025 | 1.025 | 1.241 | 1.019 | 1.020 | 0.990 | 0.990 |
| oct($ols$) | 0.955 | 1.000 | 0.984 | 0.985 | 0.922 | 0.975 | 0.983 | 0.961 | 0.987 | 0.945 |
| oct($struc$) | 1.085 | 1.094 | 1.047 | 1.018 | 0.952 | 1.027 | 1.054 | 0.981 | 1.022 | 0.953 |
| oct($wlsv$) | 1.132 | 1.137 | 1.065 | 1.059 | 0.969 | 1.050 | 1.078 | 0.989 | 1.043 | 0.960 |
| oct($bdshr$) | 1.047 | 1.085 | 1.013 | 1.011 | 0.927 | 1.009 | 1.050 | 0.966 | 1.019 | 0.942 |
| oct$_h$($bshr$) | **0.931** | 1.002 | 1.001 | 0.982 | **0.889** | **0.965** | 0.980 | 0.975 | 0.985 | 0.933 |
| oct$_h$($hshr$) | 1.081 | 1.109 | 1.039 | 1.076 | 0.973 | 1.028 | 1.061 | 0.978 | 1.052 | 0.963 |
| oct$_h$($shr$) | 1.068 | 1.088 | 1.008 | 0.995 | 0.896 | 1.023 | 1.061 | 0.966 | 1.011 | **0.924** |
| | | | $k=2$ | | | | | $k=3$ | | |
| base | 1.000 | **0.960** | 0.971 | **0.958** | 0.972 | 1.000 | **0.963** | 0.981 | **0.966** | 0.986 |
| ct($bu$) | 2.176 | 1.035 | 1.036 | 1.035 | 1.035 | 2.428 | 1.042 | 1.044 | 1.042 | 1.043 |
| ct($shr_{cs}, bu_{te}$) | 1.192 | 1.020 | **0.942** | 1.021 | 0.942 | 1.245 | 1.009 | **0.931** | 1.011 | 0.931 |
| ct($wlsv_{te}, bu_{cs}$) | 1.400 | 1.104 | 1.106 | 1.018 | 1.019 | 1.500 | 1.127 | 1.130 | 1.029 | 1.029 |
| oct($ols$) | 0.985 | 1.028 | 1.008 | 1.002 | 0.950 | 0.976 | 1.020 | 1.004 | 0.994 | 0.938 |
| oct($struc$) | 1.075 | 1.115 | 1.051 | 1.039 | 0.967 | 1.096 | 1.117 | 1.064 | 1.033 | 0.965 |
| oct($wlsv$) | 1.110 | 1.149 | 1.065 | 1.070 | 0.979 | 1.142 | 1.160 | 1.082 | 1.073 | 0.981 |
| oct($bdshr$) | 1.045 | 1.105 | 1.024 | 1.033 | 0.949 | 1.060 | 1.109 | 1.032 | 1.029 | 0.943 |
| oct$_h$($bshr$) | **0.967** | 1.029 | 1.025 | 0.998 | 0.928 | **0.954** | 1.024 | 1.025 | 0.993 | **0.911** |
| oct$_h$($hshr$) | 1.073 | 1.122 | 1.042 | 1.083 | 0.983 | 1.093 | 1.129 | 1.054 | 1.090 | 0.984 |
| oct$_h$($shr$) | 1.064 | 1.110 | 1.019 | 1.018 | **0.922** | 1.082 | 1.116 | 1.030 | 1.015 | 0.915 |
| | | | $k=4$ | | | | | $k=6$ | | |
| base | 1.000 | **0.962** | 0.987 | **0.973** | 0.996 | 1.000 | **0.963** | 0.998 | **0.984** | 1.011 |
| ct($bu$) | 2.585 | 1.052 | 1.054 | 1.053 | 1.053 | 2.849 | 1.083 | 1.085 | 1.083 | 1.084 |
| ct($shr_{cs}, bu_{te}$) | 1.277 | 1.000 | **0.923** | 1.002 | 0.923 | 1.339 | 0.999 | **0.921** | 1.000 | 0.920 |
| ct($wlsv_{te}, bu_{cs}$) | 1.559 | 1.150 | 1.153 | 1.037 | 1.037 | 1.662 | 1.189 | 1.193 | 1.066 | 1.066 |
| oct($ols$) | 0.966 | 1.022 | 1.008 | 0.994 | 0.931 | 0.962 | 1.023 | 1.014 | 1.003 | 0.930 |
| oct($struc$) | 1.106 | 1.120 | 1.076 | 1.031 | 0.963 | 1.132 | 1.132 | 1.100 | 1.039 | 0.972 |
| oct($wlsv$) | 1.157 | 1.167 | 1.097 | 1.075 | 0.982 | 1.192 | 1.187 | 1.124 | 1.090 | 0.995 |
| oct($bdshr$) | 1.065 | 1.112 | 1.041 | 1.025 | 0.939 | 1.084 | 1.121 | 1.058 | 1.029 | 0.940 |
| oct$_h$($bshr$) | **0.943** | 1.028 | 1.028 | 0.994 | **0.900** | **0.932** | 1.029 | 1.032 | 1.000 | **0.887** |
| oct$_h$($hshr$) | 1.101 | 1.137 | 1.068 | 1.093 | 0.986 | 1.126 | 1.153 | 1.089 | 1.110 | 0.999 |
| oct$_h$($shr$) | 1.089 | 1.118 | 1.039 | 1.012 | 0.910 | 1.107 | 1.118 | 1.045 | 1.006 | 0.902 |
| | | | $k=12$ | | | | | | | |
| base | 1.000 | 0.948 | 1.010 | 1.002 | 1.033 | | | | | |
| ct($bu$) | 2.990 | 1.028 | 1.031 | 1.029 | 1.029 | | | | | |
| ct($shr_{cs}, bu_{te}$) | 1.326 | **0.897** | **0.830** | **0.899** | 0.830 | | | | | |
| ct($wlsv_{te}, bu_{cs}$) | 1.679 | 1.119 | 1.123 | 1.009 | 1.009 | | | | | |
| oct($ols$) | 0.872 | 0.927 | 0.914 | 0.930 | 0.840 | | | | | |
| oct($struc$) | 1.077 | 1.028 | 1.012 | 0.950 | 0.894 | | | | | |
| oct($wlsv$) | 1.149 | 1.089 | 1.041 | 1.006 | 0.922 | | | | | |
| oct($bdshr$) | 1.021 | 1.015 | 0.964 | 0.935 | 0.855 | | | | | |
| oct$_h$($bshr$) | **0.833** | 0.927 | 0.927 | 0.927 | **0.784** | | | | | |
| oct$_h$($hshr$) | 1.066 | 1.056 | 1.005 | 1.026 | 0.926 | | | | | |
| oct$_h$($shr$) | 1.043 | 1.011 | 0.952 | 0.909 | 0.809 | | | | | |

*The Gaussian method employs a shrikage covariance matrix and includes four techniques (G, B, H, HB) with multi-step residuals.

**Table E.5:** *ES ratio indices defined in Section 5 for the Australian Tourism Demand dataset. Approaches performing worse than the benchmark (bootstrap base forecasts, ctjb) are highlighted in red, the best for each column is marked in bold, and the overall lowest value is highlighted in blue. The reconciliation approaches are described in Table 2.*

# F Computation time report

In this section, we provide a computational time analysis for the two forecasting experiments in the paper. Tables F.1 and F.2 show the runtime (in seconds) required for simulating 1000 samples (first row, base) and the additional time needed for reconciliation with various approaches in the first iteration of the experiment. The first table is refers to the Australian QNA dataset, while the second to the Australian Tourism Demand dataset. The system's hardware and software specifications are

- CPU: `Intel(R) Core(TM) i7-10700 CPU  2.90GHz 2.90 GHz`
- RAM size: `64 GB`
- R version: `R-4.2.1_2022-06-23_ucrt`
- R packages: `forecast` (Hyndman et al. 2023), `MASS` (Venables & Ripley 2002), `Rfast` (Papadakis et al. 2022), and `FoReco` (Girolimetto & Di Fonzo 2023*a*)

| **Reconciliation approach** | ctjb | $G_h$ | $H_h$ | $G_{oh}$ | $H_{oh}$ |
|---|---|---|---|---|---|
| base | 29.01 | 2.21 | 2.17 | 2.14 | 2.18 |
| ct$(shr_{cs}, bu_{te})$ | + 0.19 | + 0.13 | + 0.12 | + 0.30 | + 0.30 |
| ct$(wls_{cs}, bu_{te})$ | + 0.21 | + 0.31 | + 0.31 | + 0.33 | + 0.35 |
| oct$_o(wlsv)$ | + 0.25 | + 0.24 | + 0.22 | + 0.22 | + 0.22 |
| oct$_o(bdshr)$ | + 0.48 | + 0.44 | + 0.45 | + 0.45 | + 0.45 |
| oct$_{oh}(hshr)$ | + 0.64 | + 0.65 | + 0.64 | + 0.65 | + 0.64 |

**Table F.1:** *Computational time (in seconds) for the first iteration of the Australian QNA forecasting experiment. The first row (base) reports the time to simulate 1000 samples, and the remaining rows the additional time to reconcile them with different approaches.*

| **Reconciliation approach** | ctjb | G | B | H | HB |
|---|---|---|---|---|---|
| base | 61.21 | 660.43 | 643.54 | 641.40 | 692.63 |
| ct$(shr_{cs}, bu_{te})$ | + 3.79 | + 4.02 | + 3.79 | + 3.54 | + 4.18 |
| oct$(struc)$ | + 7.73 | + 7.10 | + 7.19 | + 7.11 | + 6.56 |
| oct$(wlsv)$ | + 8.24 | + 6.97 | + 6.99 | + 7.04 | + 6.46 |
| oct$(bdshr)$ | + 60.27 | + 52.65 | + 52.13 | + 51.92 | + 49.51 |
| oct$_h(bshr)$ | + 503.52 | + 426.20 | + 419.99 | + 418.94 | + 422.94 |
| oct$_h(hshr)$ | + 485.66 | + 482.13 | + 418.64 | + 418.82 | + 463.18 |

**Table F.2:** *Computational time (in seconds) for the first iteration of the Australian Tourism Demand forecasting experiment. The first row (base) reports the time to simulate 1000 samples, and the remaining rows the additional time to reconcile them with different approaches.*

## References


Athanasopoulos, G., Gamakumara, P., Panagiotelis, A., Hyndman, R. J. & Affan, M. (2020), Hierarchical Forecasting, *in* P. Fuleky, ed., 'Macroeconomic Forecasting in the Era of Big Data', Vol. 52, Springer International Publishing, Cham, pp. 689–719.

Athanasopoulos, G., Hyndman, R. J., Kourentzes, N. & Petropoulos, F. (2017), 'Forecasting with temporal hierarchies', *European Journal of Operational Research* **262**(1), 60–74.

Bisaglia, L., Fonzo, T. D. & Girolimetto, D. (2020), Fully reconciled GDP forecasts from Income and Expenditure sides, *in* A. Pollice, N. Salvati & F. Schirripa Spagnolo, eds, 'Book of Short Papers SIS 2020', Pearson, pp. 951–956.

Di Fonzo, T. & Girolimetto, D. (2022*a*), 'Enhancements in cross-temporal forecast reconciliation, with an application to solar irradiance forecasts', *arXiv:2209.07146* .

Di Fonzo, T. & Girolimetto, D. (2022*b*), 'Forecast combination-based forecast reconciliation: Insights and extensions', *International Journal of Forecasting, in press* .

Di Fonzo, T. & Girolimetto, D. (2022*c*), Fully reconciled probabilistic GDP forecasts from Income and Expenditure sides, *in* A. Balzanella, M. Bini, C. Cavicchia & R. Verde, eds, 'Book of Short Papers SIS 2022', Pearson, pp. 1376–1381.

Di Fonzo, T. & Girolimetto, D. (2023*a*), 'Cross-temporal forecast reconciliation: Optimal combination method and heuristic alternatives', *International Journal of Forecasting* **39**(1), 39–57.

Di Fonzo, T. & Girolimetto, D. (2023*b*), 'Spatio-temporal reconciliation of solar forecasts', *Solar Energy* **251**, 13–29.

Girolimetto, D. & Di Fonzo, T. (2023*a*), *FoReco: Point Forecast Reconciliation*. R package v0.2.6.
**URL:** *https://danigiro.github.io/FoReco/*

Girolimetto, D. & Di Fonzo, T. (2023*b*), 'Point and probabilistic forecast reconciliation for general linearly constrained multiple time series', *arXiv:2305.05330* .

Hyndman, R. J., Ahmed, R. A., Athanasopoulos, G. & Shang, H. L. (2011), 'Optimal combination forecasts for hierarchical time series', *Computational Statistics & Data Analysis* **55**(9), 2579–2589.

Hyndman, R. J., Athanasopoulos, G., Bergmeir, C., Caceres, G., Chhay, L., Kuroptev, K., O'Hara-Wild, M., Petropoulos, F., Razbash, S., Wang, E., Yasmeen, F., Garza, F., Girolimetto, D., Ihaka, R., R Core Team, Reid, D., Shaub, D., Tang, Y., Wang, X. & Zhou, Z. (2023), *forecast: Forecasting Functions for Time Series and Linear Models*. R package v8.20.
**URL:** *https://pkg.robjhyndman.com/forecast/*

Hyndman, R. J. & Khandakar, Y. (2008), 'Automatic Time Series Forecasting: The forecast Package for R', *Journal of Statistical Software* **27**, 1–22.

Hyndman, R. J., Lee, A. J. & Wang, E. (2016), 'Fast computation of reconciled forecasts for hierarchical and grouped time series', *Computational Statistics & Data Analysis* **97**, 16–32.

Ledoit, O. & Wolf, M. (2004), 'A well-conditioned estimator for large-dimensional covariance matrices', *Journal of Multivariate Analysis* **88**(2), 365–411.

Nystrup, P., Lindström, E., Pinson, P. & Madsen, H. (2020), 'Temporal hierarchies with autocorrelation for load forecasting', *European Journal of Operational Research* **280**(3), 876–888.

O'Hara-Wild, M., Hyndman, R. J., Wang, E. & Godahewa, R. (2022), *tsibbledata: Diverse Datasets for 'tsibble'*. R package v0.4.1.
**URL:** *tsibbledata.tidyverts.org*

Panagiotelis, A., Athanasopoulos, G., Gamakumara, P. & Hyndman, R. J. (2021), 'Forecast reconciliation: A geometric view with new insights on bias correction', *International Journal of Forecasting* **37**(1), 343–359.

Papadakis, M., Tsagris, M., Dimitriadis, M., Fafalios, S., Tsamardinos, I., Fasiolo, M., Borboudakis, G., Burkardt, J., Zou, C., Lakiotaki, K. & Chatzipantsiou, C. (2022), *Rfast: A Collection of Efficient and Extremely Fast R Functions*. R package version 2.0.6.
**URL:** *https://CRAN.R-project.org/package=Rfast*

Stellato, B., Banjac, G., Goulart, P., Bemporad, A. & Boyd, S. (2020), 'OSQP: An operator splitting solver for quadratic programs', *Mathematical Programming Computation* **12**(4), 637–672.

Stellato, B., Banjac, G., Goulart, P., Boyd, S. & Bansal, V. (2022), *osqp: Quadratic Programming Solver using the 'OSQP' Library*. R package v0.6.0.7.
**URL:** *osqp.org*

Venables, W. N. & Ripley, B. D. (2002), *Modern Applied Statistics with S*, 4th edn, Springer, New York.
**URL:** *https://www.stats.ox.ac.uk/pub/MASS4/*

Wickramasuriya, S. L., Athanasopoulos, G. & Hyndman, R. J. (2019), 'Optimal Forecast Reconciliation for Hierarchical and Grouped Time Series Through Trace Minimization', *Journal of the American Statistical Association* **114**(526), 804–819.